Modeling Zymogen Protein C

Lalith Perera,* Charles Foley,* Thomas A. Darden,† Darrel Stafford,‡ Timothy Mather,§ Charles T. Esmon,§ and Lee G. Pedersen*†

*Department of Chemistry, University of North Carolina, Chapel Hill, North Carolina 27599-3290; †National Institute of Environment Health Science, Research Triangle Park, North Carolina 27709; ‡Department of Biology, University of North Carolina, Chapel Hill, North Carolina 27599-3290; §Howard Hughes Medical Institute, Oklahoma Medical Research Foundation, 825 NE13, Oklahoma City, Oklahoma 73104 USA

ABSTRACT A solution structure for the complete zymogen form of human coagulation protein C is modeled. The initial core structure is based on the x-ray crystallographic structure of the γ-carboxyglutamic acid (Gla)-domainless activated form. The Gla domain (residues 1–48) is modeled from the x-ray crystal coordinates of the factor VII_a/tissue factor complex and oriented with the epidermal growth factor-1 domain to yield an initial orientation consistent with the x-ray crystal structure of porcine factor IX_a. The missing C-terminal residues in the light chain (residues 147–157) and the activation peptide residues 158–169 were introduced using homology modeling so that the activation peptide residues directly interact with the residues in the calcium binding loop. Molecular dynamics simulations (Amber-particle-mesh-Ewald) are used to obtain the complete calcium-complexed solution structure. The individual domain structures of protein C in solution are largely unaffected by solvation, whereas the Gla-epidermal growth factor-1 orientation evolves to a form different from both factors VII_a and IX_a. The solution structure of the zymogen protein C is compared with the crystal structures of the existing zymogen serine proteases: chymotrypsinogen, proproteinase, and prethrombin-2. Calculated electrostatic potential surfaces support the involvement of the serine protease calcium ion binding loop in providing a suitable electrostatic environment around the scissile bond for II_a/thrombomodulin interaction.

INTRODUCTION

Protein C (PC), a vitamin K-dependent (VKD) plasma serine protease zymogen (Mammen et al., 1960; Stenflo, 1976), is synthesized mainly in the liver and in endothelial cells (Tanabe et al., 1991) as a single chain polypeptide. The majority of the protein is converted into a two-chain disulfide-linked zymogen during secretion from the cell (Foster et al., 1990; Grinnell et al., 1991). The structure of PC is highly homologous to other VKD blood coagulation factors VII, IX, and X. However, once activated by thrombin bound to thrombomodulin on the endothelial cell surface, it functions as a natural anticoagulant (for reviews on PC and its activation, see Esmon and Esmon, 1984; Esmon, 1989, 1995a,b; Tuddenham and Cooper, 1994; Suzuki, 1995; Davie, 1995). Genetic defects in the PC pathway are associated with an increased risk for venous thrombosis (Reitsma, 1997). Deficiency of PC is one of the most common causes of an inherited autosomal dominant thrombophilia.

The zymogen (see Fig. 1) contains a pre-pro leader peptide (absent in the mature protein), a γ-carboxyglutamic acid (Gla) domain of 9 Gla residues, a short helical hydrophobic amino acid stack, two epidermal growth factor (EGF)-like domains, a linking peptide between the light chain and the heavy chain, an activation peptide, and a trypsin-like SP domain in which the catalytic triad is located at His-211(cn57), Asp-257(cn102), and Ser-360(cn195) (Fernlund and Stenflo, 1982; Stenflo and Fernlund, 1982; Foster and Davie, 1984; Foster et al., 1985, 1987). Post-translational modification removes the dipeptide Lys-156-Arg-157, so that the single chain form is converted into a two-chain molecule linked by a disulfide bond; 80% of the zymogen PC circulating in plasma is in this form (Foster et al., 1990; Grinnell et al., 1991). The activation, fluorescence properties and amidolytic activity of the single- and two-chain protein are identical (Rezaie and Esmon, 1995). Also, carboxylation of Glu residues in the amino terminal Gla domain (Stenflo, 1976; Kisiel et al., 1976), hydroxylation of an Asp residue in the EGF1 domain (Drakenberg et al., 1983; Fernlund and Stenflo, 1983) and glycosylation (McClure et al., 1992; Grinnell et al., 1991) are post-translational events.

Activation occurs when a negatively charged peptide (Lys-158-Arg-169) is released by the cleavage of the peptide bond between Arg-169 and Leu-170. Activated protein C (APC), in the presence of cofactor protein S (PS), proteolytically inactivates both factors V_a and $VIII_a$ on platelets and endothelial cells (Fay et al., 1991; Kalafatis et al., 1994). Recently, it has been shown that in addition to the function of factor V as a procoagulant after its activation by thrombin, factor V plays an important role in the anticoagulant system as a phospholipid (PL)-bound cofactor to APC (Dahlback and Hildebrand, 1994). It is also reported that factor V acts synergistically with PS as PL-bound cofactors in the presence of calcium ions (Dahlback and Hildebrand, 1994; Shen and Dahlback, 1994; Shen et al., 1997a; Dahlback, 1997). In a study using fluorescence resonance energy transfer, Yegneswaran et al. (1997) concluded that the func-

Received for publication 13 June 2000 and in final form 13 September 2000.

Address reprint requests to Dr. Lee G. Pedersen, Department of Chemistry, University of North Carolina, Chapel Hill, NC 27599-3290. Tel.: 919-962-1578; Fax: 919-962-2388; E-mail: lee_pedersen@unc.edu.

© 2000 by the Biophysical Society

0006-3495/00/12/2925/19 $2.00

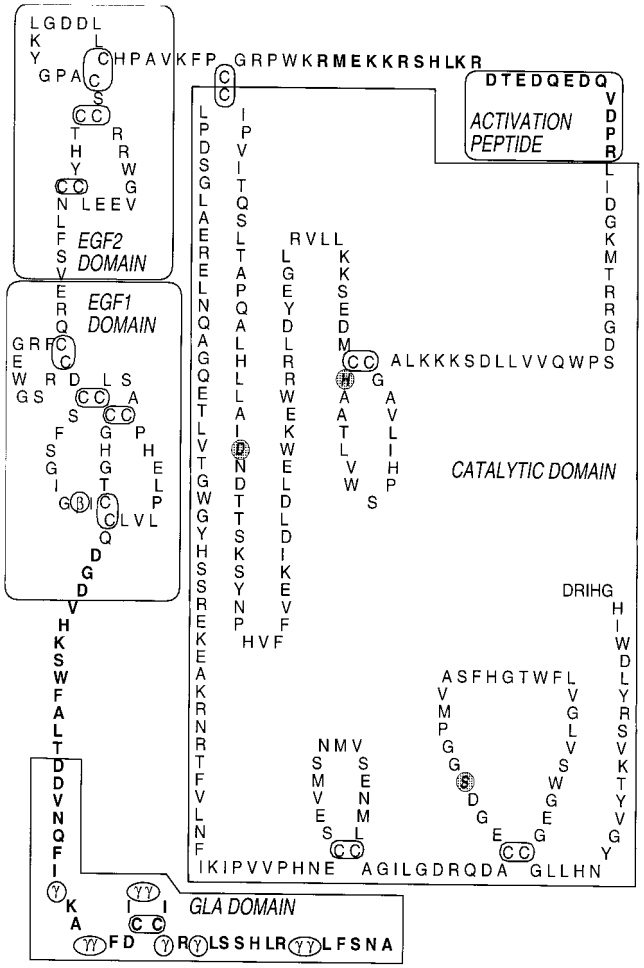

FIGURE 1 Primary amino acid sequence of human PC deduced from Foster et al. (1985). The domains are labeled according the definitions used in the text. The catalytic residues are also (*hatched*) circled. Bold-faced letters indicate the residues whose positions were initially modeled. γ, γ-carboxyglutamic acid residues; β, β-hydroxyaspartic acid.

tion of PS as a cofactor for APC is to alter the active site location of APC above the membrane surface. Yegneswaran et al. (1997) also showed that the chimera protein obtained by replacing the Gla domain of APC by that of prothrombin alters the active site location above the membrane surface. This chimera protein alone shows the same inactivation rate of factor V_a as the $APC_{wild\text{-}type}$/PS complex. Factor X_a also protects factor V_a from inactivation by APC (Nesheim et al., 1982; Jane et al., 1991). Both active and precursor forms of factor X bind to factor V_a with equal efficacy and both compete with APC for its factor V_a binding site (Jane et al., 1991). In addition to its anticoagulant activity, APC has also been shown to have profibrinolytic (Zolton and Seegers, 1973; Comp and Esmon, 1981; De Fouw et al., 1988), anti-ischemic, and anti-inflammatory (Esmon et al., 1991) activities.

The solution of the x-ray crystal structure of a significant portion of APC (Mather et al., 1996) provides an opportunity to complete the zymogen structure by theoretical techniques. Major advances of past decade in the quality of force fields (Cornell et al., 1995; Cheatham et al., 1995), molecular dynamics methodology (Essmann et al., 1995), and parallel computers make such a substantial undertaking possible. The hypothesis is that molecular dynamics (MD) simulations, if firmly based on structure, are now reasonably accurate for time scales of nanoseconds.

We have developed herein a solvent-equilibrated model for the complete zymogen PC in the presence of bound calcium ions. The initial structure is based on the 2.8 Å resolution x-ray crystal structure available for the Gla-domainless human APC (Mather et al., 1996). Homology modeling, described below in computational procedure, is used to introduce the Gla domain, the following aromatic amino acid stack, and the activation peptide. Molecular dynamics (MD) simulations are used to obtain an accurate solution structure of calcium-bound human PC. In the present model, the carbohydrate chains are not included at the four Asn-linked glycosylation sites that are post-translationally glycosylated in the circulating zymogen. Also, the post-translationally removed Lys-156-Arg-157 dipeptide in PC is present in the model, although this segment does not appear to play a role in activation (Rezaie and Esmon, 1995). Comparison of the modeled zymogen structure with the x-ray crystal structure of APC may clarify functional activities of the enzyme form. Consequently, the structural changes between the zymogen (solution model) and the enzyme (x-ray) are compared with three other zymogen/active SP systems for which x-ray crystal data are available for both zymogen and active forms. Possible functional roles of Gla and EGF1 domains and the high affinity calcium ions bound to EGF1 and SP domains are also discussed. Whereas earlier modeling work focused on the activated thrombin (II_a)-thrombomodulin (TM)-PC complex in the absence of solvent or calcium ions (Knobe et al., 1999) and on a static model that included the activation peptide and SP domain only (Fisher et al., 1994), our objective has been to obtain an accurate description for the solution structure, including state of the art dynamics, of zymogen PC in its complete calcium-bound, fully hydrated configuration. The coordinates for the model are available from the authors on request.

COMPUTATIONAL PROCEDURE

Model construction

The x-ray crystal coordinates of human APC (Protein Data Bank (pdb) entry, 1aut), along with the crystallographic water molecules, were used to model the initial structure of the zymogen form of human PC. The Gla domain and the following aromatic helical stack were absent in the x-ray crystal coordinates, as was the activation peptide. A flow chart of the model building procedure, described below in detail, is given in Fig. 2. The structure of the Gla domain of PC and the following aromatic helical stack, was constructed by replacing the necessary residues of the x-ray crystal

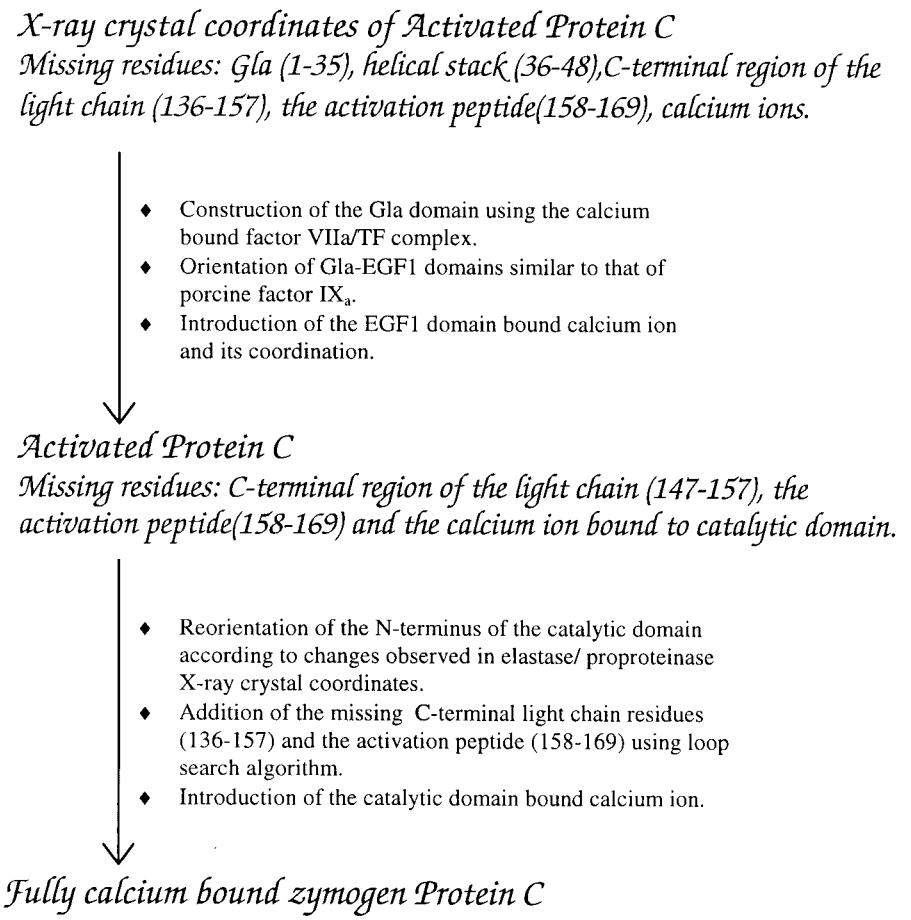

FIGURE 2 A flow chart summarizing the model construction of zymogen PC from the x-ray crystal structure (Mather et al., 1996) of calcium-free Gla-domainless APC.

structure of factor VII_a (pdb entry 1dat) using SYBYL 6.4 (Tripos, Inc., St. Louis, MO). The x-ray crystal structure of factor VII_a was determined in the presence of tissue factor (TF) and the Gla domain does, in fact, interact directly with TF, potentially causing a reorientation in the Gla-EGF1 orientation. Thus, the Gla-EGF1 orientation found in the factor VII_a/TF complex may be unique for that particular system and may not necessarily reflect the orientation of a general Gla-EGF interaction. The crystal structure is available for another VKD protein, porcine factor IX_a, but the electron density beyond the helical stack toward the N-terminus of the Gla domain was not sufficient to resolve the Gla domain structure (Brandstetter et al., 1995). In our current model, we construct the Gla segment based on the x-ray crystal structure of the factor VII_a Gla domain, but link it to the x-ray crystal structure of Gla-domainless PC so that the Gla-EGF1 orientation is similar to that of the porcine factor IX_a (pdb entry 1pfx). PC residues Gln-49,Cys-50,Cys-69-Arg-91 and factor IX_a residues Gln-50, Cys-51, and Cys-62-Leu-84 (including β-hydroxy aspartate (Hya)-71) were used in the backbone atom alignment. Also, residues in the helical stack at the C-terminal end of the Gla domain served to position the Gla domain to the Gla domainless PC. Because the Gla domain of the x-ray crystal structure of factor VII_a was mutated to create the Gla domain of PC, the relative calcium positions were preserved. Using the calcium ion coordinated to the EGF1 domain of factor VII_a as a template, a calcium ion was introduced to the Gla-EGF1 connecting region of PC. An additional calcium ion was introduced to the catalytic region (Mather et al., 1996) at a site similar to the calcium binding site in trypsin.

During activation, a 12-residue polypeptide is cleaved from the zymogen form of PC. In addition to the cleaved segment, modeling to determine the coordinates for the final 9 residues from the C-terminus of the light chain of APC (absent in the x-ray coordinate file due to disordered electron density) was necessary. The complete activation loop was added in two steps. First, it was necessary to redefine the N-terminus of the SP domain, since this fragment is inserted into the body of the protein in the structure of APC (x-ray). The N termini of available SP x-ray crystal structures in their activated forms are remarkably similar. Fortunately, x-ray crystal structures exist for the zymogen forms of several SPs; chymotrypsinogen (Wang et al., 1985), prethrombin-2 (Vijayalakshmi et al., 1994), and proproteinase E (Gomis-Ruth et al., 1995). In these zymogen structures, the backbone atoms of key residues starting at residue 20 (chymotrypsin numbering (cn)) are remarkably similar when superimposed. In Fig. 3, the N-terminal segment of the SP domains of PC, chymotrypsin (pdb entry 4cha), α-thrombin complexed with hirugen (pdb entry 1hah), porcine pancreatic elastase (pdb entry 1btu) are compared. Backbone atoms of the residues 20–25 (cn numbering) are used for the alignment. Also shown are the zymogens; chymotrypsinogen (pdb entry 2cga), prethrombin-2 complexed with hirugen (pdb entry 1hag), and proproteinase E in a ternary complex with procarboxypeptidase A and chymotrypsinogen (pdb entry 1pyt). The N-termini of the active forms of these SPs align well. The residues at position 16 in chymotrypsinogen and prethrombin-2 are found to have a similar orientation. In proproteinase E, however, residue 16 is orientationally rotated ~120°. Finally the residue at position 16 in all of the activated SP systems is found at a relative orientation of 120° to both chymotrypsinogen/prethrombin-2 and proproteinase. Thus, we were able to reconstruct the N-terminus region of the catalytic domain of the zymogen PC by overlaying it on the N-terminus of any of these three zymogen systems. We chose to reconstruct the N-terminus region of PC by using the corresponding residues of proproteinase E as a template. This choice

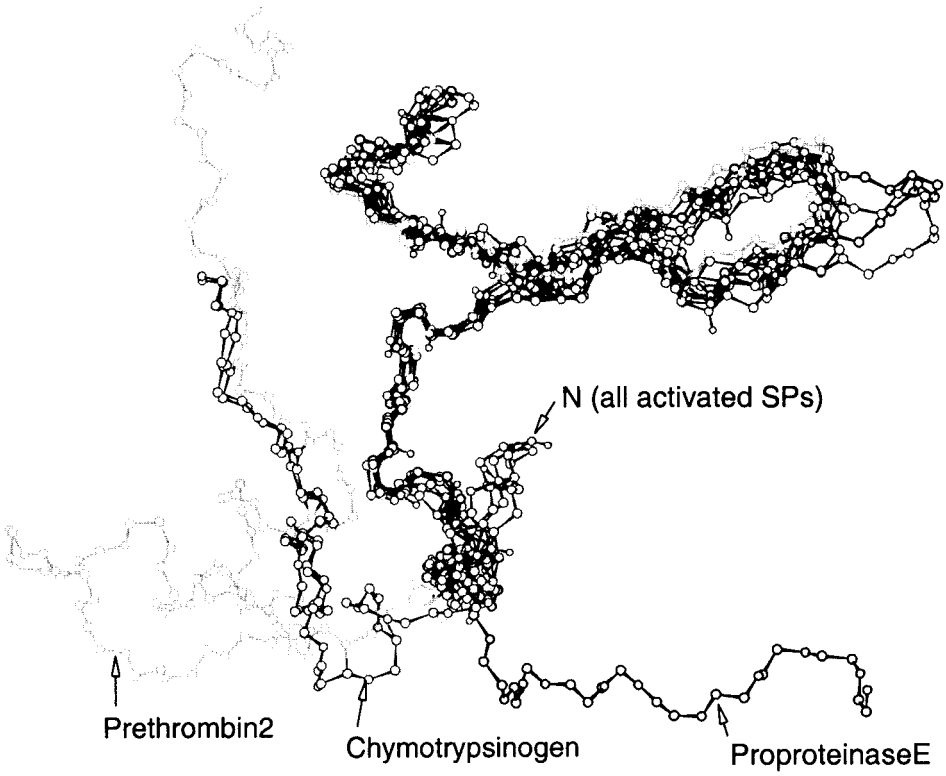

FIGURE 3 The C_a alignment of the N-terminal residues of activated serine proteases: chymotrypsin, α-thrombin, bovine pancreatic elastase, and PC. All the N-termini are well superimposed for the above active serine proteases; N labels the N-terminal C_α of the active forms. The C_α values of zymogens (prethombin-2, chymotrypsinogen, and proproteinase E) are also shown here. Alignment uses residues 20–27(cn) for all proteins. In chymotrypsinogen and prethrombin-2, the residues corresponding to the AP of PC are found to the left in the figure; the corresponding residues of proproteinase E exhibit a rotation of 120° to the right.

generally orients the initial model for the activation peptide toward the putative calcium ion binding site in the catalytic domain (see later discussion). The loop search algorithm in SYBYL6.4 Biopolymer package (Tripos) was then used to introduce the AP between the C-terminus of the light chain and the N-terminus of the catalytic domain. Twenty-five different loops were generated, of which 10 appeared reasonable. Of these, a conformation that presented the pre-PC linking dipeptide (Lys-156-Arg-157) as well as the scissile activation bond well exposed was chosen. This conformation accommodates interaction of the AP with residues that directly coordinate the SP domain bound calcium ion. All necessary hydrogen atoms were added using the Protonate module of AMBER 5.0 (Case et al., 1997).

Simulation protocol

We initially energy minimized the structure around the PC/factor IX Gla domain splice point (residues 34–46) and the structure surrounding the calcium ion bound to the EGF1 domain, since part of the helical stack (residues Ser-42, Asp-46, and Asp-48) contacts this calcium ion. Since the remainder of the protein structure was based on the energy minimized x-ray crystal structure, no additional segment-wise energy minimization runs were necessary for backbone refinements. However, energy minimization of the side chains was employed (500 steepest descent steps followed by 10,000 conjugate gradient steps). The protein (along with the crystallographic water molecules and the calcium ions) was then solvated in a box of water molecules so that the box boundaries were at least 12.5 Å away from any protein atom. Water molecules used in the solvation of the protein for which the oxygen or hydrogen atoms were within 2.0 Å of any atom in the protein were excluded. The central simulation box contained 409 residues of the zymogen PC, 25,010 water molecules, and 9 calcium ions. In addition to the calcium ions, six sodium ions were introduced as free non-protein-bound counterions. These counterions did not coordinate with any of the protein residues at any time during the MD simulation. The simulation system was thus electrically neutral. The total number of atoms in this box was 81,399. In the first step, only the added water molecules and counterions were energy minimized at constant volume (10,000 conjugate gradient steps), then all atoms except the protein were subjected to energy minimization (another 10,000 conjugate gradient steps) and finally, the whole system was energy minimized (10,000 conjugate gradient steps). All atoms except those of the protein were subsequently subjected to a slow heating procedure to bring the temperature of the system to 300 K. In this heating procedure, the temperature of the system was raised by 50° at a time in seven intervals of 1.5 ps each. After 25 ps of a constant volume-constant temperature MD simulation, the system was reminimized (5000 conjugate gradient steps). After another heating run of 10 ps to bring the temperature back to 300 K, a constant-temperature-constant volume MD run was performed for 25 ps. Finally, a constant pressure-constant temperature protocol was adopted to simulate 2900 ps of MD.

In the present study, we used the second generation of AMBER force field (Cornell et al., 1995) in conjunction with the particle mesh Ewald method (Essmann et al., 1995) to accommodate long range interactions in all of the solution simulations. The TIP3P model was used to represent the water molecules. The MD trajectory calculations were done with AMBER version 5 (Case et al., 1997). Non-bonded cutoff for the direct sum was chosen to be 8.0 Å. The time step was 1 fs with the nonbonded interactions updated at every step. This choice of updating nonbonded interactions and the periodical removal of the translational and rotational motions of the center of mass (at every 2.5 ps) prevents artifacts such as the "flying ice cube" (Harvey et al., 1998).

RESULTS AND DISCUSSION

Global aspects of the simulation

Our model for the zymogen form of human PC in solution is based on the x-ray crystal structure of APC (Mather et al.,

1996). The Gla domain, the helical stack following the Gla domain, the AP, and the calcium ions were aligned to the x-ray crystal structure based on homology considerations. The production runs were performed at constant pressure and constant temperature. The density of the system was found to fluctuate around 0.996 g/cc during the final 500 ps of the 2.9-ns trajectory.

The root mean square deviations (RMSDs) of backbone atoms from their initial positions ($t = 0$ ps) have been used to measure the stability of the simulation and to provide insight into possible structure fluctuations (Hamaguchi et al., 1992; Li et al., 1996; Perera et al., 1997). The RMSDs for the complete protein and for certain selected substructural domains are presented in Fig. 4. The evaluation of RMSDs of substructural domains is carried out after aligning appropriate residues from a conformation at time t, with that at $t = 0$ ps. For example, only Gla domain residues are used for alignment in the calculation of RMSD for that domain. The sharp rise observed during the first 800 ps in the RMSD of all residues tends to flatten out but is subject to transient fluctuations. The magnitude of this RMSD curve, however, does not continue to increase for the final 2000-ps segment, implying that the protein structure is stable over this time scale. Individual domains show relatively smaller RMSDs and fluctuations. Small fluctuations around the average values over the complete time period of 2900 ps is an indication of stable secondary structure.

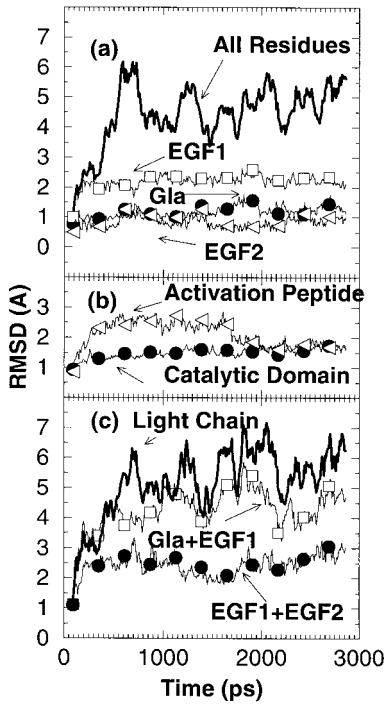

FIGURE 4 The root mean square deviations (RMSDs) of the backbone atoms. (*a*) All amino acid residues (*dark solid line*), the Gla residues 1–35 (*filled circles*), the EGF1 residues 48–92 (*open triangles*) and the EGF2 residues 93–136 (*open squares*). (*b*) The AP (residues including the connecting region; 137–169) (*open triangles*) and the SP domain (residues 170–409) (*filled circles*). (*c*) Combined Gla/EGF1 region (residues 1–91) (*open squares*), combined EGF1/EGF2 region (residues 48–136) (*filled circles*) and the entire light chain (residues 1–136) (*dark solid line*).

We conclude that on the 3-ns time scale there are no significant structural changes when going from crystal to solution. The EGF1 domain displays slightly larger magnitude in RMSD. Similar large RMSD is found in the initial 1500 ps for the AP. The final 1-ns segment of the AP is remarkably flat, implying that this region has reached its equilibration during the first 1500 ps of dynamics. Although the initial segment of the RMSD of the EGF1 domain rises sharply during the first 200 ps, an eventual stabilization is observed for this domain. Since part of the EGF1 domain (second disulfide loop containing a Hya residue) was necessarily modeled, it is not surprising that the early time RMSD values were elevated. Likewise, the significant changes to the coordinates of the N-terminus residues of the EGF1 domain, modeled so as to align the Gla-EGF1 orientation consistent with that of factor IX_a, contribute to early time RMSDs. Residues 137–169 (including AP residues 158–169) show somewhat larger fluctuations during the first 1500-ps segment, but these become subdued during the latter part of the trajectory. In general, domain-domain movements are apparent in that the RMSDs increase as domains are jointly considered (RMSD of light chain $>$ RMSD of {Gla + EGF1} or {EGF1 + EGF2} $>$ RMSD of Gla or EGF1 or EGF2).

The relative dynamics of individual residues (α-carbons) that may not contribute to observable reorganization in secondary structure can be investigated by computing the atomic B-factors (York et al., 1994) using the variance, $\langle \Delta r^2 \rangle$, in the simulations through the relationship $B = [8\pi^2/3]\langle \Delta r^2 \rangle$). The simulation B-factors were calculated using the coordinates of the last 200-ps segment of the MD trajectory (Fig. 5). Since there is a tumbling of the molecule within the central box, one must first remove this motion in obtaining the average structure during the last 200 ps. The simulation B-factors were computed by two different procedures; first by optimally aligning all backbone atoms with those of the $t = 0$ ps configuration (shown in solid lines) and secondly by aligning backbone atoms of each domain with the corresponding atoms of the $t = 0$ ps configuration (shown in dotted lines). It is clear that the latter procedure is desired if domain-domain movement takes place. Relatively smaller B-factors are apparent for the catalytic domain (residues 170–409), indicating a stable solution structure for this domain for the zymogen form (Fig. 5 *b*). Although not exact, the experimental pattern for the peak positions is largely conserved in the calculated B-factors indicating the atoms with large motion in the x-ray crystal structure remain mobile during the simulation. The patterns in the calculated B-factors remain the same regardless of the two methods used to calculate them, but the calculations performed using the entire molecule for alignment show

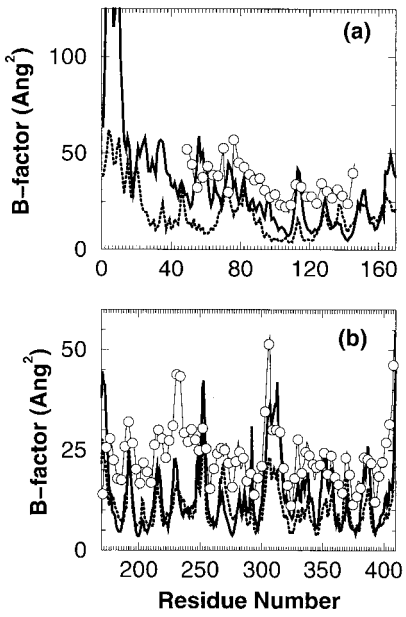

FIGURE 5 B-factors calculated for backbone C_α-atoms using the last 200-ps segment of the MD trajectory. (*a*) Light chain. (*b*) SP domain. The B-factors were calculated by using the entire protein as a template for alignment (*dark solid lines*) or after aligning individual domains and combining data (*dotted line*). The domain definitions are given in the text. X-ray B-factors are also shown (*open circles*). Interdomain motion, unless removed, confounds B-factor evaluation.

slightly elevated B-factors. The segment 1–12 (Ω-loop residues) at the N-terminus of the light chain shows relatively large B-factors if the entire molecule is used in the alignment. There is a noticeable shift, however, in the baseline from the N-terminal Gla region to the end of EGF1 domain. This shift is not observed when the B-factors are calculated using the alignment of individual domains. This baseline shift originates from the interdomain motion among Gla, EGF1, and EGF2 domains. Relatively larger peaks observed in the dotted curve may be attributed to the intradomain rearrangements. For example, the Ω-loop as a region can move without yielding a large perturbation to the Gla domain because of its protruding arrangement and, indeed, this region shows larger B-factors. The same is true for the central region of EGF1 domain where several residues are involved in the binding of a calcium ion.

Light chain

The light chain of PC (Fig. 6 *a*) consists of three domains: Gla (residues 1–37, Fig. 6 *b*), EGF1 (residues 49–91, Fig. 6 *c*), and EGF2 (residues 92–136, Fig. 6 *d*). A helical stack (residues 37–48) connects the Gla domain to the first EGF domain. The residues of this stack participate in the coordination of the calcium ion bound to the first EGF1 domain. Following the EGF2 domain, a 21-residue peptide (residues 137–157) connects the EGF2 domain to the activation peptide (residues 158–169). This 21-residue peptide chain is also linked to the SP domain through a disulfide bond.

The Gla domain and the helical stack (residues 1–47) were missing from the N-terminal region in the x-ray crystal structure of human APC (Mather et al., 1996). Since the reported 3-D structure was of the activated form, the AP is also absent (residues 158–169) and, due to diffuse electron density, a peptide fragment from the C-terminal region of the light chain was missing (residues 147–157). We reconstructed the missing portions in our simulated protein using homology modeling. The stability of the individual domains can be examined by computing the differences between the backbone α carbon positions in the initial and the final configurations after 3-D alignments. In Fig. 7 *a*, the deviations of C_α positions are measured by aligning a given domain structure at the final configuration to the corresponding domain structure at $t = 0$ ps. On the average, most residues remain near their initial C_α positions (deviations around 1 Å). Smaller deviations occur for the residues in the EGF2 domain. The segments that exhibit appreciable C_α deviations include the N-terminal region of the EGF1 domain (residues 47–56). This region involved considerable modeling to generate the structure, particularly for the calcium ion in the EGF1 domain. The C_α deviations can also be used as a measure for the domain separations. In Fig. 7 *b*, each domain of the final solution structure is aligned separately to the corresponding domains of the solution structure at $t = 0$ ps. We display the curves after separate helical stack, EGF1 and EGF2 alignments. Once the helical stack (residues 34–48) is aligned (dark solid line), domain motions in both sides are visible via their increased C_α distances. Similar behavior is observed for EGF1 (dotted line) and EGF2 (light solid line) alignments. We conclude that the Gla, EGF1, and EGF2 domains have relative movements during the trajectory, but each largely retains an individual domain structure similar to the initial structure.

The Gla, EGF1, and EGF2 domains do not directly interact via hydrogen bonds or salt bridges. Only the residues in the connecting regions make direct hydrogen bonds with the residues in the adjacent domains. Flexibility around the connecting region results, though the integrity of the individual domains are maintained. Even though there is interdomain motion, the length of the protein is relatively unaltered, because the motions are largely around the long axis of the molecule.

In the initial modeling, the Gla-EGF1 orientation of porcine factor IX_a was used to orient the Gla domain of PC with its EGF1 domain. However, in the final structure of PC, an orientation distinct from that of factor IX_a is observed. The light chain of PC, when compared with the corresponding segments of factors VII_a (in the TF-bound form) and IX_a, has evolved to a shape between that of the light chain of elongated factor VII_a and of curved factor IX_a.

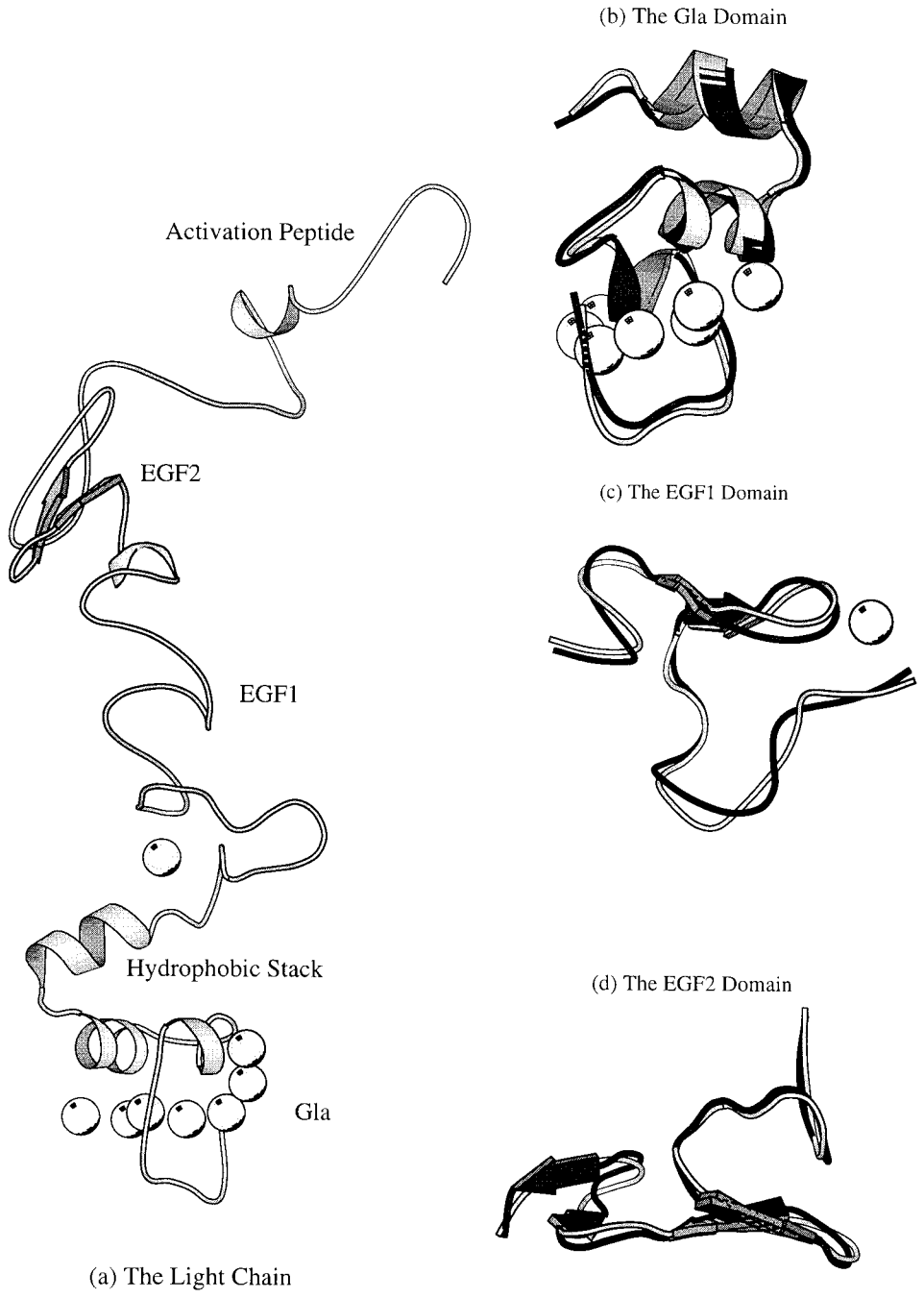

FIGURE 6 (*a*) The light chain backbone structure created from the last snapshot at $t = 2900$ ps of the trajectory. Calcium ions; light solid spheres. The Gla and EGF1 domains stack vertically; the EGF2 domain is positioned perpendicular to the hypothetical long axis of Gla and EGF1 domains. The SP domain (not shown) positions on top of the EGF2 domain. (*b*) The Gla domain backbone structure generated at $t = 0$ ps (*dark tube*) is superimposed with the final snapshot of the backbone atoms (*light tube*) of the Gla domain. The calcium ions correspond to the final structure. (*c*) Same comparison as in *b*, but for the EGF1 domain. (*d*) Same comparison as *b*, but for the EGF2 domain. All figures are generated using the program Molscript (Kraulis, 1991).

Gla domain

The Gla domain of human PC was modeled by making necessary amino acid residue substitutions to the x-ray crystal structure of factor VII_a (Banner et al., 1995, 1996) calcium and TF bound, pdb entry 1dan. The calcium and crystal water molecules were retained unmodified. In the initial configuration, in which the Gla-EGF1 orientation is similar to the x-ray crystal factor IX_a-assumed alignment, there are no direct hydrogen bonds, van der Waals contacts or salt bridges among the residues of the two domains. As has been indicated by the smaller magnitudes and fluctuations in the RMSD as well as the small deviations of C_α positions, the secondary structure of the Gla domain is not altered from its original form (see Fig. 6 *b*, in which the Gla domains of PC in the final structure and factor VII_a are compared).

The Ω-loop and the unique H-bond network at Ala-1, which is tucked into the interior of the protein and makes H-bonds with residues Gla-16, Gla-20, Ile-21 and Gla-26, is maintained. Also, the Gla-calcium network that is found in the structure of the Gla domains of VKD proteins (pro-

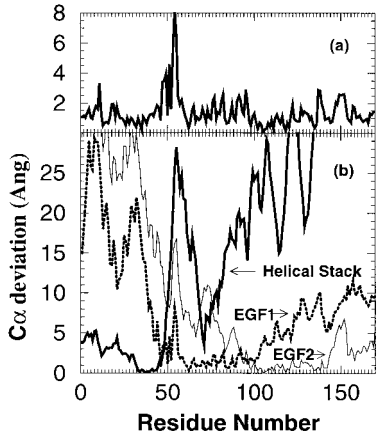

FIGURE 7 (*a*) Deviations of α-carbons of the corresponding light chain residues in the active and zymogen (solution model) structures after optimal alignments. Each domain is separately aligned. (*b*) C_α deviations for the corresponding residues in the active and zymogen forms after aligning only one domain at a time. Domain alignments are shown by *dark solid line*, the helical hydrophobic stack (residues 35–48); *dotted line*, the EGF1 domain (residues 48–91); and *light solid line*, the EGF2 domain (residues 92–136).

thrombin and factor VII_a) is well-preserved in the present simulation. Of the seven calcium ions present in contact with Gla residues, four have two or fewer coordinations with water molecules. The remaining three Gla residues, which are more solvent accessible, are coordinated with three or more water molecules throughout the trajectory calculation. The three hydrophobic residues (Phe-4, Leu-5, and Leu-8) in the Ω-loop extend away from the protein, oriented for potential insertion into the lipid membrane.

Compared to the other VKD blood coagulation proteins, human PC has a low PL (phosphatidylserine/phosphatidylcholine) binding affinity ($K_d \sim 1500$ nM). Bovine PC and human and bovine factor VII_a have been shown to have even lower binding affinities toward lipid surfaces ($K_d >$ 15,000 nM; McDonald et al., 1997a,b; Shen et al., 1997b). It has been proposed (Shen et al., 1997b) that the lower affinity of bovine PC is largely due to the presence of proline at position 10 in place of His in human PC. However, in an experiment in which the first 46 residues in the N-terminal region of PC is replaced by that of factor VII (Geng and Castellino, 1997), the activated form of the modified protein was found to be very similar to that of its wild-type counterpart in plasma anticoagulant activity, as well as activity toward inactivation of coagulation factor $VIII_a$. All VKD coagulation proteins except factor VII and PC contain a Gla residue in position 33. McDonald et al. (1997) suggest that position 33 which is occupied by either Gln (in PC) and Arg (in factor VII), may be responsible for the low binding affinities. Also, the mutation of Ser-11, a residue unique to human PC (in all other VKD coagulation proteins it is Gly), to Gly yields increased membrane affinity (Shen et al., 1998). The residues discussed above are highlighted in Fig. 8. Assuming that the lipid binding of the Gla domain is through a combined mechanism of PL insertion of Phe-4, Leu-5, and Leu-8 (Christiansen et al., 1994, 1995a; Christiansen and Castellino, 1994; Jalbert et al., 1996) and calcium bridging, one can assign the calcium ion plane to be coplanar with the lipid head groups. Given this conformation, His-10 could have an increased interaction strength with the anionic lipid head groups since it can be positively charged. Conversely, Ser-11 is placed so that it blocks any incoming lipid headgroup from bridging with a nearby calcium ion. Such a situation would reduce calcium ion exposure with the charged lipid head groups, thereby possibly reducing the lipid binding affinity of human PC.

Gla-26-Lys is a functionally defective mutation in human PC found in the plasma of patients with hereditary thrombophilia (Nishioka et al., 1996). This mutant exhibits lowered activation rates and anticoagulant activity. Even though defective APC and normal APC both displayed similar PS binding, defective PC and its activated form do not bind to phospholipids or cultured human endothelial cells. The finding of Nishioka et al. (1996) suggests that a Gla-26-dependent conformation is required for the binding of PC or APC to PL membrane, the II_a/TM complex and the

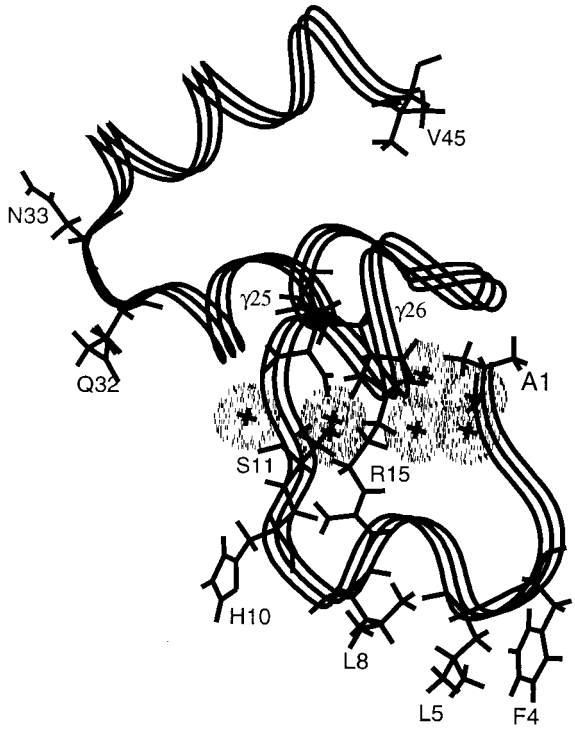

FIGURE 8 A snapshot of the Gla domain (zymogen) viewed perpendicular to the helical hydrophobic stack (residues 35–48) at $t = 2900$ ps. Important residues described in the text are marked using the stick representation of bonds. The solid spheres represent the calcium ions. γ, γ-carboxyglutamic acid.

surface of endothelial cell PC/APC receptor, but not for PS interactions. In the zymogen PC conformation, we find that Gla-26 is substantially involved in the Gla-calcium network apparently required for membrane binding (Colpitts et al., 1995). It is directed toward the interior of the protein where several of the buried calcium ions are located, forming four ionic bonds with three different calcium ions. Gla-26, along with Gla-7, Gla-16, and Gla-29, coordinates three calcium ions, whereas the other Gla residues have only one or two calcium ions in their coordination shells. Particularly, Gla-26, in concert with Gla-7 and Gla-16, may play an indirect role on the formation of the Ω-loop, since all bind to a calcium ion that is in the immediate solvation shell of Ala-1. Since the initial calcium ion positions were obtained from the x-ray crystal structure of FVII/TF complex, and the Gla residues are well preserved between FVII and PC, and also based on our previous computational work on factor IX calcium positioning that was used to guide the NMR experimental data (Li et al., 1997), we are confident that the calcium positions in our model after 3 ns may be near to what one might find in the actual system.

The location of the active site of membrane-bound APC relative to a PL surface has been determined using fluorescence resonance energy transfer (Yegneswaran et al., 1997). In the absence of PS, the distance is found to be 94 ± 3 Å. The incorporation of PS, however, reduced this distance to 84 Å. Subsequent addition of PS did not change the distance of the active site from the lipid surface for factors X_a, IX_a, and VII_a. The reduction in distance was attributed to the cofactor function that apparently relocates the active site of APC. In the present simulation, the active site of the zymogen form of PC is about 89 Å above the hypothetical membrane surface. To provide this conservative estimate, we assume that the calcium ion plane resides on the membrane surface for bridging interactions and the three hydrophobic residues (Phe-4, Leu-5, and Leu-8) are inserted into the lipid membrane.

EGF1 domain

The main function of the EGF domains is likely to provide protein-protein or protein-cell interactions (Hogg et al., 1992). Cheng et al. (1997) evaluated the importance of the functional interactions of the EGF1 residues of PC with activators and substrates. They noted through mutational studies that the charged residues of the EGF1 domain and the calcium ion binding site maintain the structural integrity of this module but these residues have little direct functional interaction with activators or substrates. Also, the calcium ion binding to the Gla domain does not seem to be influenced by calcium ion binding to the EGF1 domain (Geng et al., 1996; Cheng et al., 1997).

The EGF1 domain of PC differs somewhat from the corresponding domain of other VKD coagulation proteins, with the presence of an additional small loop (residues 59–63) created by a disulfide bond. This domain shows the largest RMSD among the individual domains present in the light chain (Fig. 4), but the alignment of the x-ray crystal and solution backbone structures (Fig. 6 *c*) does not reveal any global restructuring in this domain. The C_α deviations (Fig. 7) for the EGF1 domain indicate that a significant contribution to the RMSD for this domain may arise from residues 52–57. Also, above average C_α deviations are found in the region bracketing Hya-71. The calcium ion present near the EGF1 domain (recall that we have modeled and equilibrated this structural element) is doubly coordinated with Hya-71 through two side chain carboxylate oxygens. The only other residue from the EGF1 domain to coordinate this calcium ion is Ile-73, via the backbone carbonyl oxygen. Ser-42, Asp-46, and Asp-48 from the connecting region between Gla and EGF1 domains also coordinate with this calcium. One stable water molecule is found in its coordination shell (Fig. 9 *a*). This calcium ion maintains a stable eight-member coordination shell. As was seen in the model of factor VII_a (Perera et al., 1999), the geometry of the expanded coordination shell is a pentagonal bipyramid in which carbonyl O of Ser-42, OD2 of Asp-46, both OD1 and OD2 of Hya-71, and carbonyl O of Ile-73 define the pentagon; a water O is located at the bottom vertex. OD1 and OD2 of Asp-48 share the other vertex. The equatorial oxygen distances are found within 2.1 to 3.1 Å of the neighboring ligands and the top and bottom vertex oxygens maintain their distances to other complexing oxygens between 3.0 and 3.8 Å. The water oxygen distances are biased toward larger values, indicating that the calcium ion maintains a one-sided, glove-like network with the protein atoms. The EGF1 calcium ion appears to provide a pivot point for Gla-EGF1 relative motion. In contrast, the SP domain bound calcium ion (Fig. 9 *b*) is tightly surrounded by 7 ligand oxygens in a square-bipyramidal environment throughout the simulation.

Christiansen et al. (1995) showed that the helix-breaking mutation of Ser-42-Pro results in a ~35% reduction in anticoagulant activity of APC (Christiansen et al., 1995b). In an assessment of the role of the helical stack (residues 34–43), substitution of the helical stack of PC by that of factor IX did not result in substantial changes in the Gla domain-related calcium-dependent properties, suggesting that the helical structural element plays a more important role than the specific amino acids. The backbone of the peptide fragment containing Hya-71 remains perpendicular to the helical stack axis of hydrophobic residues (see Fig. 6 *a*). If we assume our present model, and if the hydrophobic residues Phe-4, Leu-5, and Leu-8 do insert themselves into the PL surface, then the Gla and EGF1 domains can be viewed as a cylindrical column built on the inserted residues. We have observed a relative motion between the Gla and EGF1 domains throughout the simulation. Interestingly, we found smaller relative Gla-EGF1 motion in our simulation study for the light chain of factor VII_a (Perera et al.,

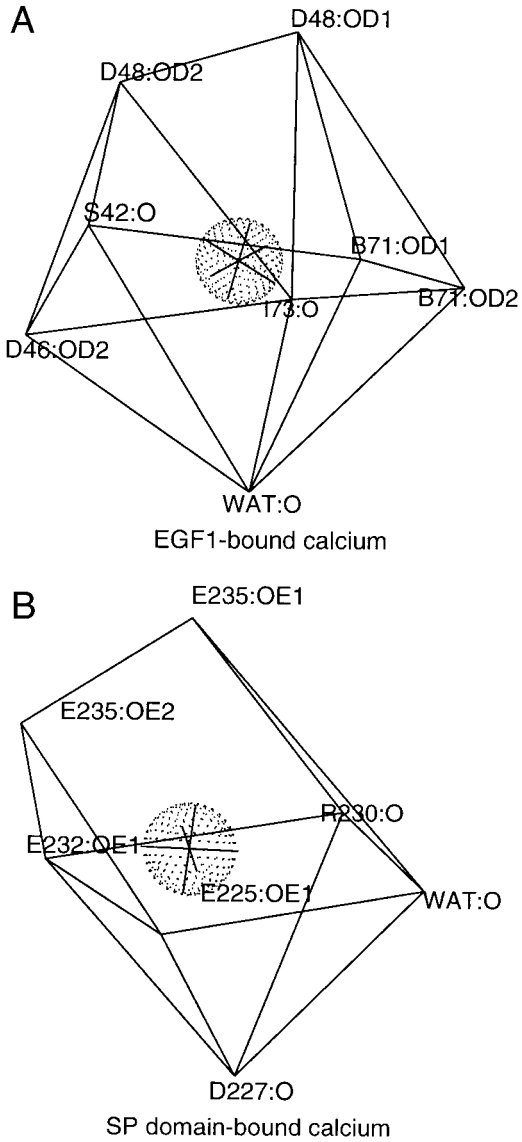

FIGURE 9 The final zymogen structure coordination spheres of the high affinity calcium ions bound to (*a*) the EGF1 domain and (*b*) the SP domain.

1999) in the absence of TF. The EGF1-bound calcium ion and its coordinating residues are not in direct contact (no salt bridges or hydrogen bonds) with residues that bind to the calcium ions of the Gla domain. Thus, the simulation structure is consistent with the experimental work of Cheng et al. (1997), who concluded that no significant influence on calcium ion binding of the Gla domain is found due to the EGF1 calcium binding. Finally, the bulk of the EGF1 domain residues made no hydrogen bonds or salt bridges with the neighboring Gla and EGF2 domains. However, Arg-91 in the connecting region between the EGF1 and EGF2 domains maintains strong contacts with both Glu-85 (in EGF1) and Asp-101 (in EGF2). The lack of a number of significant contacts with neighboring domains, however, suggests the possibility of relatively low energy torsional motions near the domain connecting regions.

EGF2 domain

The EGF2 domain (Fig. 6 *d*) is a stable region that does not appear to undergo significant restructuring during the activation process. In fact, except for a few residues in the N-terminal connecting region, most EGF2 residues exhibit C_α deviations smaller than 1.0 Å from the x-ray crystal structure (Fig. 7). In addition to the hydrogen bonds found in the activated form of the x-ray crystal structure (Asn-102/Arg-286, His-107/Thr-371, Tyr-108/Leu-278, and Cys-109/Arg-286) between the EGF2 and SP domains, a hydrogen bond evolves between the EGF2 and SP domains of the predicted solution structure of the zymogen form (Asp-101/His-369). Despite the nearness of EGF2 to the catalytic domain, direct contacts are limited.

Activation peptide (AP)

The AP of PC is the shortest (only 12 residues from Asp-158 to Arg-169) of the VKD proteins that release an AP. It contains 6 acidic residues and only one basic (Lys) residue, and is therefore highly negatively charged. On the other hand, the segment connecting the AP to the EGF2 domain (residues 137–157) contains 8 Lys and Arg residues and only one acidic Glu residue (charge = +7e). This situation creates a remarkable dipolar environment for this segment of this protein. In fact, bovine PC carries only four Asp residues whose charge is counterbalanced by two basic residues present in the AP region, making this region still a slightly acidic one. Still, the 23 amino acid residues that connect the AP with the EGF2 domain of bovine PC contain 10 Lys and Arg residues to one Glu (charge = +9e). APs of both human and bovine forms of factors IX (35 AP residues) and X (52 AP residues) are 3 to 4 times larger than that of PC and contain an excess of 6 to 10 acidic residues. For factors IX and X, the amino acid residues connecting the AP to the EGF2 domain contain an excess of only 3 or 4 basic residues. Such differences among PC and other VKD proteins in charge distributions around the scissile bond may require different conditions for the initial approach of the zymogen to its enzyme for its activation. For example, thrombin alone can activate PC but activation rates are increased by at least 1000-fold in the presence of TM. TM may thus enhance the electronegative environment around the active site of thrombin. In this section, we analyze the predicted structure of the AP (158–169) along with the linker peptide (residues 137–157) that connects the EGF2 domain to the AP. Despite the fact that this segment is modeled, RMSDs were found to be comparable with the other regions. Fig. 10 provides a snapshot (at $t = 2.9$ ps) of

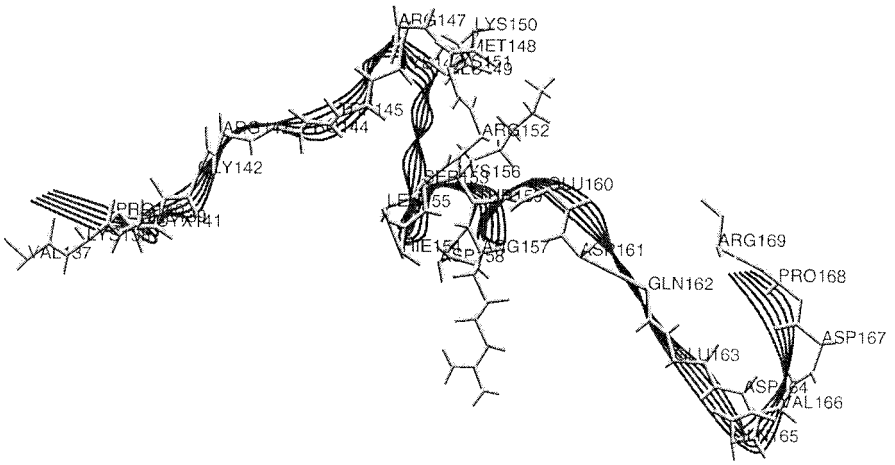

FIGURE 10 The activation peptide (residues 158–169) along with the connecting region (residues 146–157) that follow the EGF2 domain. The backbone (*ribbon*) at t = 0 ps and the backbone atoms (*sticks*) at t = 2900 ps are displayed.

this region along with the backbone ribbon of the initial configuration (t = 0 ps).

PC is activated by II_a bound to TM on endothelial cells (Esmon et al., 1993). Positively charged groups near the catalytic site cleft of thrombin may directly interact with the negatively charged AP in PC activation. Mutations of several acidic residues in or near active cleft of thrombin (Glu-217(cn)-Ala, Glu-192(cn)-Gln, and Glu-39(cn)-Lys) result in increased II_a/PC interactions but have a little effect on those with II_a/TM (Le Bonniec and Esmon, 1991; Le Bonniec et al., 1991; Rezaie and Esmon, 1993). Mutations of the acidic residues either to basic or neutral residues increase the electropositivity of the electrostatic surface around the thrombin catalytic cleft and favorably accommodate the negatively charged AP residues adjacent to the scissile bond through enhanced electrostatic interactions. Such movement would require the cleavage site of the AP of zymogen PC to be exposed to the incoming thrombin (or the II_a/TM complex). The AP cleavage site is readily available for such interactions in the present simulation structure (solvent accessibilities are 114 and 107 Å^2 for Arg-169 and Leu-170, respectively). However, the P1′ (Arg-169) residue in the current final configuration has its side chain in a salt bridge with Glu-232 in the calcium binding loop; this interaction must complete with the P1′-S1′ interaction that purportedly occurs at the active site of II_a.

In the present model, several H-bonds are found between the AP and SP domains including several with the calcium ion binding residues in the SP domain. Both Arg-229 and Arg-230 of the SP domain interact with Asp-167 of the activation peptide through H-bonds. Rezaie and Esmon (1992) observed a twofold decrease in the maximum calcium-dependent fluorescence quenching due to the mutation of Asp residues (to Gly) found at P3 (Asp-167) and P3′ (Asp-172) positions (scissile bond = Arg-169—Leu-170). Our simulation shows that Asp-167 can actively participate in the stabilization of the SP calcium ion binding loop. Also, in our current model Asp-172 interacts with Arg-314 via a strong salt bridge. Similarly, Lys-233 interacts with both Asp-161 and Glu-163. This network enhances the availability of acidic residues in the calcium ion binding loop (residues 225–235) for their calcium ion binding function by moving side chains of the basic residues in this loop away from the acidic residues. In addition, Trp-231 and Gln-165 also form a H-bond. Although the current simulation is of benchmark size and duration, complete exploration of the AP conformations may require a longer time scale than can be simulated with current computer capabilities.

Serine protease (SP) domain

Because a major aim of the present simulation is to estimate a reasonably accurate structure for the solution form of the calcium-bound zymogen, comparison of the SP domain of the modeled zymogen form with its crystallized activated form may be useful in obtaining information about restructuring that must occur near the catalytic residues on activation.

The SP domain of human PC consists of 240 residues. The three most important residues (His-211, Asp-257, and Ser-360, rendered in Fig. 11) define the functional role of a SP. It is common, in SP domains of both coagulant and anticoagulant SPs in the blood coagulation cascade, to observe the same global fold. The catalytic residues are located at the junction between two interconnected six-stranded β-barrel domains. The SP domain of PC, along with trypsin, coagulation factors II, VII, IX, and X, possess a calcium ion binding site.

In modeling the SP domain for the zymogen form of PC, two major modifications to the x-ray crystal configuration of the activated form were introduced. Structural similarities found among the crystal configurations of the SPs in the blood coagulation cascade in their active and zymogen forms were used in the creation of the N-terminal connection to the AP. All hemostatic proteases circulate in blood in

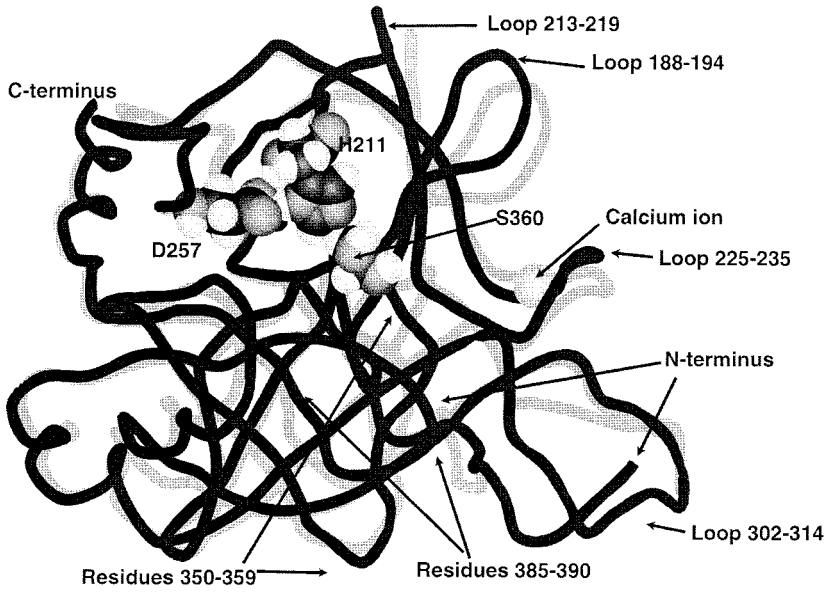

FIGURE 11 The catalytic domains of PC in the zymogen model (*dark line*) and the active x-ray crystal structure (*light line*). Catalytic residues in the zymogen model structure are rendered. Also, loops with observed movements (APC → PC) in the backbone structure are labeled.

the inactive zymogen form and become active due to specific cleavage after Arg-15(cn) in the SP. Several VKD coagulation proteins (PC, factors IX and X) contain two cleavage sites, and the removal of a small peptide takes place during the process of their activation. Once cleaved, the newly created N-terminus of the SP domain becomes embedded in the SP interior. This structural element apparently facilitates the charge transfer from Asp-102(cn) via His-57(cn) to Ser-195(cn) required for PC catalytic activity. In the zymogen x-ray crystal structure of proproteinase E (and for two other zymogens considered), the N-terminal residues of the catalytic domain points away from the protein with activation leading to insertion of the N-terminus near the active site. The structure of proproteinase E was adopted for the modeling of the N-terminal connecting region of PC (the structure of three residues, Leu-170(cn16), Ile-171(cn17), and Asp-172(cn18), are adapted by this implementation), thereby introducing a significant change to the SP domain of the APC template. Secondly, a calcium ion, which is critical for zymogen activity, was introduced to the region described in the literature (Mather et al., 1996). We shall analyze the structural consequences of these modifications.

As has been seen from Fig. 4, the RMSDs (zymogen versus APC) calculated for the SP domain are small and comparable with those of Gla and EGF2 domains indicating a relatively stable solution structure (see also Fig. 11). Considering that PC is in the zymogen form with no inhibitor present in the simulation (as opposed to the x-ray crystal structure of APC with inhibitor present), this result is rather unexpected. The RMSDs suggest that rearrangement in the N-terminal region of the SP domain of APC does not lead to large changes in the overall solution structure. There are, however, differences in the side chain orientations (PC versus APC) and several loops undergo movement.

The side chain motion can be studied with the help of B-factors calculated for side chain heavy atoms. In Fig. 12, we plot the side chain B-factors of the SP domain residues averaged over the final 200 ps of the trajectory. The configurations at each picosecond were aligned with the $t = 0$ ps structure, and B-factors were then calculated for all heavy atoms. Side chain B-factors of each residue were calculated by averaging over all side chain heavy atoms present. The experimental B-factors (averaged over the side chain heavy atoms of each residue) are also given in Fig. 12 for comparison. The backbone B-factors (Fig. 5) calculated from simulation are smaller in magnitude than the corresponding B-factors calculated in x-ray experiments while the computed side chain B-factors from the simulation show either comparable or larger magnitudes than the x-ray experiment. It is reasonable that the solvent environment may lead to larger thermal fluctuations that translate to larger B-factors (than experiment) observed for side chains in the simulation. The general pattern of fluctuations in the calculated B-factors of the zymogen, however, is similar to that observed in the x-ray crystal structure for APC. The solvent accessibilities (and their changes) are shown in Fig. 12 to ascertain whether there is a correlation between the B-factors and the solvent accessibilities. The changes in the solvent accessibility (ΔSAA = SAA in the solution structure (zymogen) − SAA in the x-ray crystal structure (activated)) can identify residues that are newly exposed to the solvent or new interactions that may accompany activation. The patch containing three Lys residues, Lys-191(cn37) to Lys-193(cn39), has large B-factors and also large solvent accessibilities. This segment is recognized to be crucial for

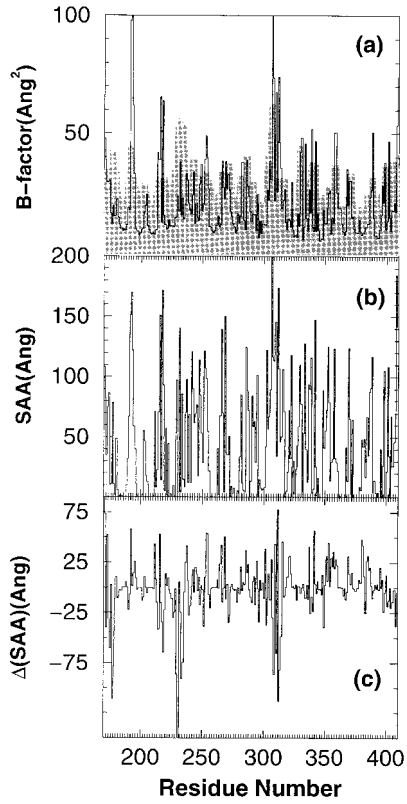

FIGURE 12 (*a*) Side chain B-factors averaged over the heavy atoms of side chains of each residue of the catalytic domain (*solid line*) are compared with those from the x-ray crystal structure of APC (*shaded histograms*). (*b*) Solvent-accessible areas and (*c*) changes in the solvent-accessible areas in going from zymogen to APC $\{\Delta(\mathrm{SAA}) = \mathrm{SAA}_{\mathrm{zymogen}} - \mathrm{SAA}_{\mathrm{APC}}\}$.

activation by II_a/TM complex but not by II_a alone (Gerlitz and Grinnell, 1996). Though all of these Lys residues are highly solvent accessible, once activated, Lys-192(cn38) loses part of its solvent exposure. In another positively charged patch of residues, Lys-217(cn62) and Lys-218(cn63) show large side chain B-factors along with high solvent accessibilities in zymogen PC. Upon activation, these two residues become even more solvent-exposed (for Lys-217(cn62) from 172 to 206 Å^2 and for Lys-218 from 94 to 158 Å^2). In the zymogen model Lys-217(cn62) forms a H-bond with neighboring residue Ser-216(cn61) and Lys-218(cn63) makes H-bonds with Leu-219(cn64) and Asp-239(cn84). In the x-ray crystal form (APC), both are unbound.

Cation binding to the SP domain

Rezaie et al. (1992) reported that the binding of the calcium ion at the high affinity binding site in the SP domain of PC results in a conformational change that is required for activation by the II_a/TM complex (Rezaie and Esmon, 1992; Rezaie et al., 1992). This calcium ion binding site was predicted to be near the 10 residue loop from Glu-225(cn70) to Glu-235(cn80) (Mather et al., 1996). This segment closely follows the structure of the calcium ion binding loop of trypsin (Bode and Schwager, 1975). In our initial modeled structure, the calcium ion was introduced to a six-center coordination environment by ligating it with OE1 of Glu-225(cn70), OE1 of Glu-232(cn77), OE1 and OE2 of Glu-235(cn80), carbonyl oxygens of Asp-227(cn72), and Arg-230(cn75). A seventh ligation position was occupied by a water molecule as the simulation progressed. The coordination shell of the calcium ion bound to the SP domain is more compact than that observed for the EGF1-domain bound calcium ion (see Fig. 9b). Mutation of Glu-235(cn80)-Lys results in a form that no longer requires calcium for rapid activation by the II_a/TM complex (Rezaie et al., 1994). Presumably the calcium ion binding site is disrupted. This mutation may, however, favorably change the electrostatic potential around this putative calcium site for incoming II_a/TM complex, much as the calcium ion does in the wild-type structure. It remains to be shown if occupancy of a calcium ion in this site is required for physiological functioning of APC (He and Rezaie, 1999).

PC activation is also upwardly regulated by sodium ion binding (He and Rezaie, 1999). He and Rezaie (1999) identified a loop in APC similar to the sodium ion binding loop of thrombin, and concluded that this loop may be allosterically linked with the divalent cation binding loop of the protease. We find that the sodium ion binding region predicted by He and Rezaie (1999), residues 385–390(cn221–225), is strongly electronegative via electrostatic potential surface computations (not shown). This loop (residues 385–390) is remote from the putative calcium binding site and we find no residues simultaneously shared by both putative ion binding sites. We find, however, that the putative sodium ion binding site is near the scissile bond of PC activation (within 10 Å). Thus, sodium ion binding to this site could modulate the electrostatics around the scissile bond, thereby enhancing the interaction of the active site cleft of thrombin. Further computational studies are currently under way in our laboratory to elucidate the effect of this sodium ion on the SP domain structure.

Comparison of PC/APC with other known zymogen/active SP pairs

C_α deviations for the solution zymogen model and x-ray crystal structure of APC for the SP domain are given in Fig. 13. The residues that had crystal contacts with neighboring APC molecules in the crystal configuration are marked in this figure along with the residues that had inhibitor contacts. Since the crystal contacts and inhibitor contacts are removed in our solution model structure of the zymogen, the residues that participated in contacts relax to yield somewhat larger C_α deviations (x-ray crystal APC x-ray versus

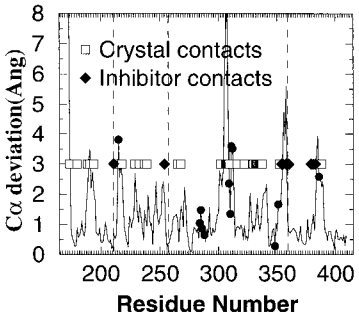

FIGURE 13 Deviations of the α-carbon atoms of the corresponding SP domain residues of PC in the zymogen form and the active form after the best alignment. PC numbering is used. Residues with crystal contacts (*open squares*) and inhibitor contacts (*diamond*) in the x-ray crystal configuration of the active form are marked. *Filled circles* indicate the presence of additional residues (in APC) if aligned with chymotrypsin.

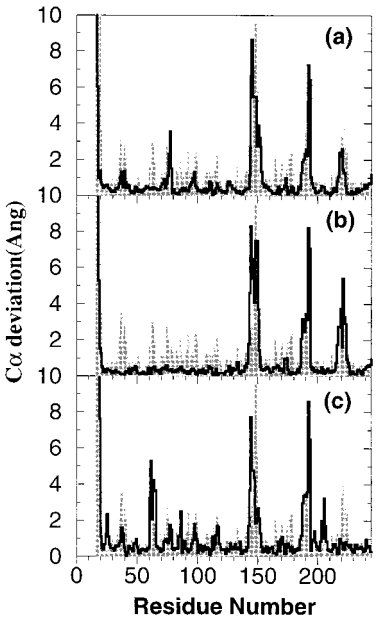

FIGURE 14 Comparison of the C_α deviations of PC (active versus zymogen; *shaded histogram*) and (*a*) chymotrypsin/chymotrypsinogen, (*b*) α-thrombin/prethrombin-2, and (*c*) elastase/proproteinase systems (*dark solid lines*). The backbone atoms of residues 24–238(cn) are used to align the zymogen with its active form.

solution PC). On the other hand, for more than half (133) of the residues, including two of the catalytic triad residues, His-211(cn57) and Asp-257(cn102), in the SP domain have C_α deviations <1 Å and only 48 residues (20% of the total in this domain) have values >2 Å. The broad peak that brackets residues 301–313(cn142–158) is likely due to removal of crystal contacts, as most of the residues become exposed to the solvent upon solvation. Other residues with large deviations participate in forming hydrogen bonds and salt bridges with the residues in the AP or the reconstructed N-terminal part of the catalytic domain, for example, hydrogen bonds and salt bridges between Asp-167-Asn-313(cn150), Asp-172(cn18)-Arg-314(cn151), and Lys-174(cn20)-His-303(cn144)). Residues 350–358(cn186–183) and 383–389(cn219–224) contribute to peaks in the C_α deviations. These segments are linked by a disulfide bridge, are near the 301–315(cn142–152) loop, and bracket residues that have inhibitor contacts and crystal contacts in the x-ray crystal structure. The segment 385–390(cn221–225) is the putative sodium ion binding site and the absence of a sodium ion in the current simulation may contribute to some disorder. Almost all regions that show elevated C_α deviations contain residues exposed to solvent. Thus, differential solvation apparently provides the most significant contribution to the C_α deviations observed in the present simulation.

The C_α deviations between PC (modeled) and APC (x-ray) are compared (Fig. 14) with three other zymogen/activated SP protein pairs for which the structures exist: a) chymotrypsin (pdb entry 2cga)/chymotrypsinogen (pdb entry 4cha), b) prethrombin-2(pdb entry 1hag)/α-thrombin (pdb entry 1hah) (both active and zymogen forms are complexed with hirugen), c) bovine proproteinase E (pdb entry 1pyt)/porcine pancreatic elastase (pdb entry 1btu). The active site residues are already in their activated conformations in all of the activated systems, as is the case of PC. Once the SP domain residues of PC are aligned with the homologous residues of chymotrypsin, additional residues of PC that do not have corresponding residues in chymotrypsin are found. These inserted residues are marked in Fig. 13 (dark circles in five separate segments). In Fig. 14, only the first residue in each group was used to facilitate the comparison. Removal of the C_a deviations corresponding to these inserted residues from the plot does not change the general characteristics of the plot (compare Figs. 13 and 14). Thus, the inserted residues of PC do not appear to alter the structure common to these SP domains. The overall picture that emerges from these comparisons is that the deviations in the C_a values (PC versus APC) are similar to the three available SP pairs.

Once superimposed, the backbone positions of the catalytic triad residues of PC in the simulation structure are essentially indistinguishable from the x-ray crystal structure (RMSD of 0.5 Å) of APC. Comparison of the x-ray crystal structures of the other zymogen/active SP pairs shows the same fixed structure for catalytic triad residues. Unaltered catalytic triad backbone atom positions among the activated and zymogen serine proteases imply that during activation, the local environment around the preformed catalytic triad in the zymogen form of PC undergoes electrostatic and steric changes suitable for enzymatic function. Such local changes could provide the specificity of the enzymatic reaction to a particular serine protease.

In the systems for which x-ray crystal data are available, the loop cn186–194 has been proposed (Blow and Steitz, 1970) to play a key role in regulating enzyme activity. In the

active state, the N-terminus of the SP domain turns inward after cleavage and interacts via a salt bridge with Asp-194(cn), a neighbor of the catalytic residue Ser-195(cn) (Blow and Steitz, 1970). A similar situation is observed for APC: Leu-170(cn16) contacts Asp-359(cn194), also through a salt bridge(Mather et al., 1996). The carboxylate group and the amido nitrogen of Asp-194 in chymotrypsin (Wang et al., 1985) and other SPs have an observable rotation (approximately 140°) around the C_α-C bond of Asp-194(cn) between zymogen and active forms (see Fig. 15, *a-c*).

We initiated the PC simulation at a conformation similar to the activated protein. Under normal simulation conditions, it is not unreasonable to expect that an extremely long trajectory calculation would be necessary to complete all of the conformational changes in PC that are similar in magnitude to the three experimental systems (zymogen/activated pairs). Currently available computational resources cannot handle such lengthy simulations. Ultimately, improvements in sampling techniques may speed this process. We observe a small rotation for the carboxylate group and the amido nitrogen of Asp-194 (about 27°) during the first 1500 ps of the simulation (Fig. 15 *d*). Increase in the solvent accessibilities of the neighboring residues to Asp-194(cn) occurs. The C_α deviations at $t = 1500$ ps indicate that structural changes are underway and in a direction leading to steric hindrance of the substrate binding site. The rate of the Asp-194(cn) conformational change may be down-regulated by the Asp-194(cn) (side chain)/Cys-356(cn191) (backbone) H-bond in the activated form and/or by the

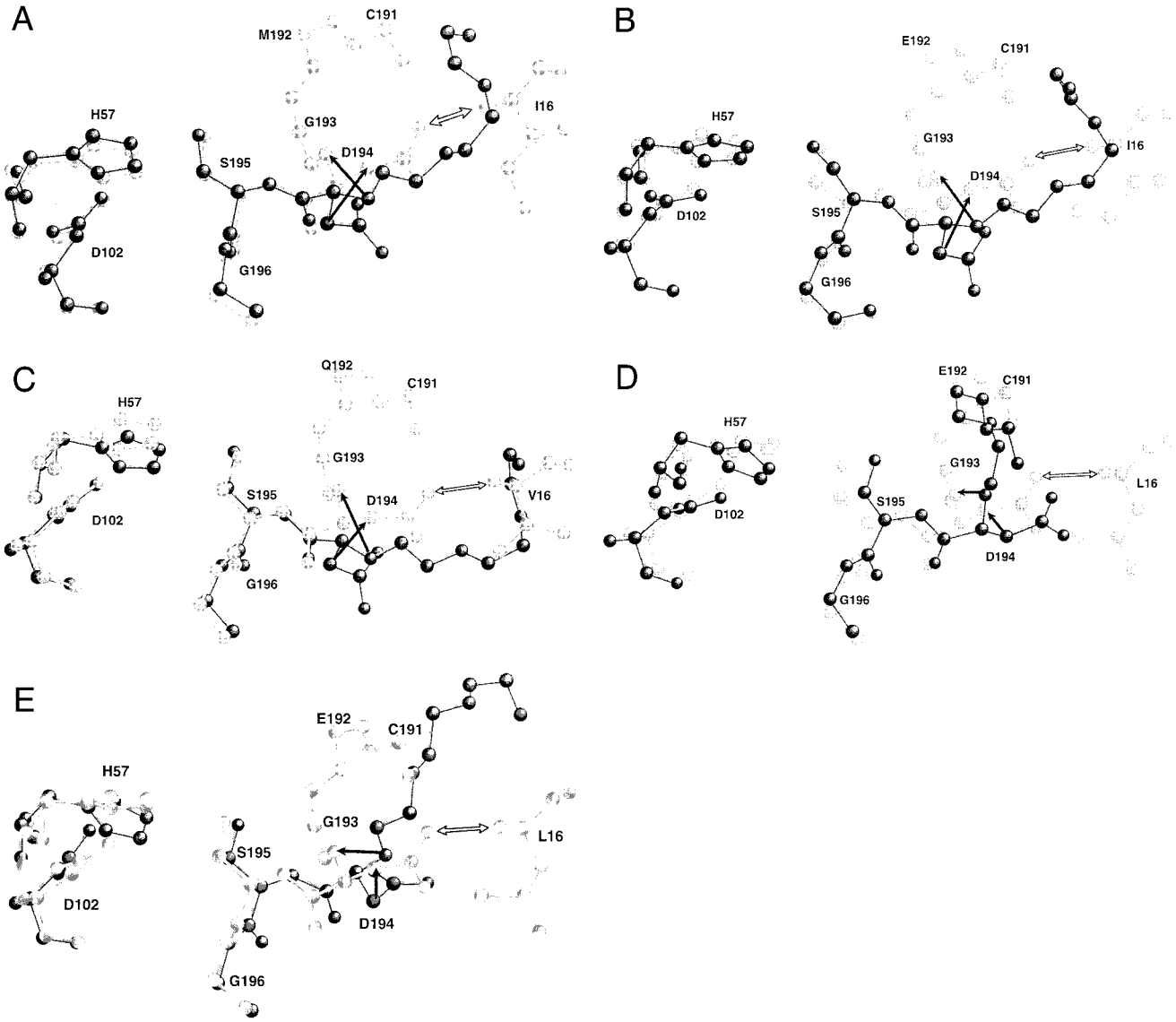

FIGURE 15 Rearrangements around the s_1 specificity pockets after zymogen activation: zymogen (*dark tracing*) and active protease (*light tracing*). (*a*) Chymotrypsin/chymotrypsinogen. (*b*) Thrombin/prethrombin-2. (*c*) Elastase/proproteinase E. (*d*) APC/PC at $t = 1500$ ps. (*e*) APC/PC at $t = 2900$ ps.

water molecules H-bonded to the protein. The time scale of these refolding events may require a much more lengthy simulation before the penultimate conformational changes are observed. We subsequently forced this reverse transition (activated during the 1500- to 1600-ps segment of the trajectory) through step-wise constrained dynamics. All constraints were relaxed after 1600 ps. Such a forced change might have led to large positional fluctuations. The system, however, responded favorably to this implemented change, and no aberrations were observed in the following dynamics, e.g., no large fluctuations in RMSD or B-factors. Changes in the relative energies of the system before and after this transformation are indistinguishable from the noise level. The final configuration is given in Fig. 15 *e*. It corresponds well with the zymogen orientations of this fragment in the three experimental zymogen structures.

Because of the observed differences in substrate specificity, it is reasonable to expect dissimilarities near the specific binding pockets. For instance, Met-192 of chymotrypsin moves from a deeply buried position in the zymogen to the surface in the active form. In contrast, the SAA of Glu-357(cn192) decreases from 124 $Å^2$ in zymogen PC to 88 $Å^2$ in APC. All the neighboring residues in APC similarly have decreased SAAs. The region of the substrate binding site in chymotrypsin that accommodates aromatic and bulky nonpolar groups is not fully formed in its zymogen (see Fig. 15 *a*). Fig. 15 *e* displays that in the predicted zymogen form of PC, the loop comprising residues 186–194(cn) restricts the accessibility of the active site. This is consistent with the chymotrypsin/chymotrypsinogen case. The "oxyanion hole" at the catalytic serine side chain required to stabilize the proposed tetrahedral transition state in chymotrypsin is incomplete in chymotrypsinogen (Stryer, 1988). The same is true for the other two pairs as well as for our final solution model of PC. Analysis of the APC and chymotrypsin x-ray crystal structures yields similar structural arrangements around the catalytic serine.

Activation

Electrostatic potential surfaces can be useful in alignment of interacting regions for incoming molecules. Specifically, large electropositive or electronegative regions can reasonably attract oppositely charged entities through long-range electrostatic interactions. The analysis of the calculated electrostatic potential surfaces of the enzyme and substrate separately may guide the relative alignment of the substrate/enzyme complex. We have evaluated the electrostatic potential surface of the calcium-bound PC zymogen model (our substrate) using the popular code Grasp (Nicholls et al., 1991; results not shown). Electrostatic potential surfaces of the II_a/TM complex (pdb entry 1dx5) and II_a alone, after removing TM from the II_a/TM complex, were also calculated.

The picture that emerges for the formation of the catalytic complex from consideration of the structures and their electrostatic potential surfaces is as follows. The active site cleft of II_a is relatively electronegative. The concentration of acidic residues near the PC scissile bond naturally imposes a barrier for interaction with the active site of II_a. Due to the SP calcium ion, Glu residues in the loop become interior residues, while basic residues in this loop become exposed and partially neutralize the acidic residues around the scissile bond. Likewise, the basic residues in the fragment connecting the AP to the EGF2 domain similarly provide additional charge balancing for suitable II_a interaction. We find that, viewed externally via Grasp, the scissile bond region is actually positive. In fact, the comparison of the electrostatic potential surfaces of the II_a/TM complex with bare II_a after TM is removed, shows significant enhancement in the electronegativity around the II_a catalytic site due to TM. Since the binding of TM does not induce marked allosteric structural changes in the vicinity of IIa catalytic site (Fuentes-Prior et al., 2000), the increase of the negative electrostatic potential around the catalytic site of II_a could provide proper positioning of PC for its activation by II_a/TM. Thus, the electrostatic potential surfaces via Grasp are useful in providing an overview of complementarity that accompanies the PC/IIa/TM complex formation.

SUMMARY

An equilibrated solution structure for the completely calcium-coordinated inactive zymogen form of human coagulation protein C is developed. The initial structure is based on x-ray crystallographic structure of the Gla-domainless activated form. The Gla domain (residues 1–48) is modeled from the x-ray crystal coordinates of the factor VII_a/TF complex and oriented with the EGF1 domain to yield an orientation consistent with the x-ray crystal structure of porcine factor IX_a. The missing C-terminal residues in the light chain (residues 147–157) and the AP (residues 158–169) are introduced using homology modeling. MD simulations (Amber-particle-mesh-Ewald) are used to approximate the complete calcium-complexed solution structure. The individual domain structures of PC in solution are largely unaffected by solvation, whereas joint domains show relative movement during the trajectory. However, the estimated height of the active site of the zymogen form above the membrane plane is within the experimental estimates. The Gla domain structure is similar to that of the factor VII_a; thus, it may be reasonable to conclude that the two proteins should show similar lipid binding properties. The EGF1 and catalytic domain bound calcium ions in the predicted solution structure show expanded and tightly bound coordination shells, respectively.

Except for the N-terminal region of the catalytic domain, the backbone atoms of the other catalytic domain residues in active and zymogen forms yield a close alignment (RMSD of 1.4 Å). The catalytic triad residues show a close backbone alignment for zymogen and active forms. The loop

comprising residues 347–359(cn186–194) moves (active → zymogen) so as to reduce access to the active site. The positioning of the AP and the presence of the catalytic domain bound calcium ion facilitate the electrostatics of II_a/TM interactions in PC activation.

This work was supported by National Institutes of Health grant HL-06350 (to L. G. P.). We acknowledge the computational resources provided by the North Carolina Supercomputing Center, National Cancer Institute, the Pittsburgh Supercomputing Center. We acknowledge a grant from the National Science Foundation for computational resources. We are grateful to Mr. Vance Shaffer of IBM for assistance.

REFERENCES

Banner, D. W., A. D'Arcy, C. Chene, F. Vilbois, W. H. Konigsberg, A. Guha, Y. Nemerson, and D. Kirchhofer. 1995. The crystal structure of the complex of human factor VIIa with human soluble tissue factor. *Thromb. Haemost.* 73:1183–1183.

Banner, D. W., A. D'Arcy, C. Chene, F. K. Winkler, A. Guha, W. H. Konigsberg, Y. Nemerson, and D. Kirchhofer. 1996. The crystal structure of the complex of blood coagulation factor VIIa with soluble tissue factor. *Nature.* 380:41–46.

Blow, D. M., and T. A. Steitz. 1970. X-ray diffraction studies of enzymes. *Annu. Rev. Biochem.* 39:63–100.

Bode, W., and P. Schwager. 1975. The refined crystal structure of bovine beta-trypsin at 1.8 A resolution. II. Crystallographic refinement, calcium binding site, benzamidine binding site and active site at pH 7.0. *J. Mol. Biol.* 98:693–717.

Brandstetter, H., M. Bauer, R. Huber, P. Lollar, and W. Bode. 1995. X-ray structure of clotting factor IXa: active site and module structure related to Xase activity and hemophilia B. *Proc. Natl. Acad. Sci. USA.* 92: 9796–9800.

Case, D. A., Pearlman, D. A., Caldwell, J. W., Cheatham, T. E. III, Ross, W. S., Simmerling, C. L., Darden, T. A., Merz, K. M., Stanton, R. V., Cheng, A. L., Vincent, J. J., Crowley, M., Ferguson, D. M., Radmer, R. J., Siebel, G. L., Singh, U. C., and Kollman, P. A. AMBER 5. 1997. University of California, San Francisco.

Cheatham, T. E. III, J. L. Miller, T. Fox, T. Darden, and P. A. Kollman. 1995. Molecular dynamics simulations on solvated biomolecular systems: the particle mesh Ewald method leads to stable trajectories of DNA, RNA, and proteins. *J. Am. Chem. Soc.* 117:4193–4194.

Cheng, C. H., J. P. Geng, and F. J. Castellino. 1997. The functions of the first epidermal growth factor homology region of human protein C as revealed by a charge-to-alanine scanning mutagenesis investigation. *Biol. Chem.* 378:1491–1500.

Christiansen, W. T., and F. J. Castellino. 1994. Properties of recombinant chimeric human protein C and activated protein C containing the gamma-carboxyglutamic acid and trailing helical stack domains of protein C replaced by those of human coagulation factor IX. *Biochemistry.* 33: 5901–5911.

Christiansen, W. T., J. P. Geng, and F. J. Castellino. 1995b. Structure-function assessment of the role of the helical stack domain in the properties of human recombinant protein C and activated protein C. *Biochemistry.* 34:8082–8090.

Christiansen, W. T., L. R. Jalbert, R. M. Robertson, A. Jhingan, M. Prorok, and F. J. Castellino. 1995a. Hydrophobic amino acid residues of human anticoagulation protein C that contribute to its functional binding to phospholipid Vesicles. *Biochemistry* 34:10376–10382.

Christiansen, W. T., A. Tulinsky, and F. J. Castellino. 1994. Functions of individual gamma-carboxyglutamic acid (Gla) residues of human protein c. Determination of functionally nonessential Gla residues and correlations with their mode of binding to calcium. *Biochemistry.* 33: 14993–15000.

Colpitts, T. L., M. Prorok, and F. J. Castellino. 1995. Binding of calcium to individual γ-carboxyglutamic acid residues of human protein C. *Biochemistry.* 34:2424–2430.

Comp, P. C., and C. T. Esmon. 1981. Generation of fibrinolytic activity by infusion of activated protein C in dogs. *J. Clin. Invest.* 68:1221–1228.

Cornell, W. D., P. Cieplak, C. I. Bayly, I. R. Gould, K. M. Merz, Jr., D. M. Ferguson, D. C. Spellmeyer, T. Fox, J. W. Caldwell, and P. A. Kollman. 1995. A new force field for molecular mechanical simulation of nucleic acids and proteins. *J. Am. Chem. Soc.* 117:5179–5197.

Dahlback, B. 1997. Factor V and protein S as cofactors to activated protein C. *Haematologica.* 82:91–95.

Dahlback, B., and B. Hildebrand. 1994. Inherited resistance to activated protein C is corrected by anticoagulant cofactor activity found to be a property of factor V. *Proc. Natl. Acad. Sci. USA.* 91:1396–1400.

Davie, E. W. 1995. Biochemical and molecular aspects of the coagulation cascade. *Thromb. Haemost.* 74:1–6.

De Fouw, N. J., R. M. Bertina, and F. Haverkate. 1988. Activated protein C and fibrinolys. *In* Protein C and related proteins. R.M.Bertina, editor. Longman Group UK, Churchill Livingstone. 71–90.

Drakenberg, T., P. Fernlund, P. Roepstorff, and J. Stenflo. 1983. beta-Hydroxyaspartic acid in vitamin K-dependent protein C. *Proc. Natl. Acad. Sci. USA.* 80:1802–1806.

Esmon, C. T. 1989. The roles of protein C and thrombomodulin in the regulation of blood coagulation. *J. Biol. Chem.* 264:4743–4746.

Esmon, C. T. 1995b. Inflammation and thrombosis: the impact of inflammation on the protein C anticoagulant pathway. *Haematologica.* 80: 49–56.

Esmon, C. T. 1995a. Inflammation: they're not just for clots anymore. *Curr. Biol.* 5:743–746.

Esmon, C. T., and N. L. Esmon. 1984. Protein C activation. *Semin. Thromb. Hemost.* 10:122–130.

Esmon, C. T., N. L. Esmon, B. B. Le, and A. E. Johnson. 1993. Protein C activation. *Methods Enzymol.* 222:359–85:359–385.

Esmon, C. T., F. B. J. Taylor, and T. R. Snow. 1991. Inflammation and coagulation: linked processes potentially regulated through a common pathway mediated by protein C. *Thromb. Haemost.* 66:160–165.

Essmann, U., L. Perera, M. L. Berkowitz, T. Darden, H. Lee, and L. G. Pedersen. 1995. A smooth particle mesh Ewald method. *J. Chem. Phys.* 103:8577–8593.

Fay, P. J., T. M. Smudzin, and F. J. Walker. 1991. Activated protein C-catalyzed inactivation of human factor VIII and factor VIIIa. Identification of cleavage sites and correlation of proteolysis with cofactor activity. *J. Biol. Chem.* 266:20139–20145.

Fernlund, P., and J. Stenflo. 1982. Amino acid sequence of the light chain of bovine protein C. *J. Biol. Chem.* 257:12170–12179.

Fernlund, P., and J. Stenflo. 1983. Beta-hydroxyaspartic acid in vitamin K-dependent proteins. *J. Biol. Chem.* 258:12509–12512.

Fisher, C. L., J. S. Greengard, and J. H. Griffin. 1994. Models of the serine protease domain of the human antithrombotic plasma factor activated protein c and its zymogen. *Prot. Sci.* 3:588–599.

Foster, D., and E. W. Davie. 1984. Characterization of a cDNA coding for human protein C. *Proc. Natl. Acad. Sci. USA.* 81:4766–4770.

Foster, D. C., M. S. Rudinski, B. G. Schach, K. L. Berkner, A. A. Kumar, F. S. Hagen, C. A. Sprecher, M. Y. Insley, and E. W. Davie. 1987. Propeptide of human protein C is necessary for gamma-carboxylation. *Biochemistry.* 26:7003–7011.

Foster, D. C., C. A. Sprecher, R. D. Holly, J. E. Gambee, K. M. Walker, and A. A. Kumar. 1990. Endoproteolytic processing of the dibasic cleavage site in the human protein C precursor in transfected mammalian cells: effects of sequence alterations on efficiency of cleavage. *Biochemistry.* 29:347–354.

Foster, D. C., S. Yoshitake, and E. W. Davie. 1985. The nucleotide sequence of the gene for human protein C. *Proc. Natl. Acad. Sci. USA.* 82:4673–4677.

Fuentes-Prior, P., Y. Iwanaga, R. Huber, R. Pagila, G. Rumennik, M. Seto, J. Morser, D. R. Light, and W. Bode. 2000. Structural basis for the anticoagulant activity of the thrombin-thrombomodulin complex. *Nature.* 404:518–525.

Geng, J. P., and F. J. Castellino. 1997. Properties of a recombinant chimeric protein in which the gamma- carboxyglutamic acid and helical stack domains of human anticoagulant protein C are replaced by those of human coagulation factor VII. *Thromb. Haemost.* 77:926–933.

Geng, J. P., C. H. Cheng, and F. J. Castellino. 1996. Functional consequences of mutations in amino acid residues that stabilize calcium binding to the first epidermal growth factor homology domain of human protein C. *Thromb. Haemost.* 76:720–728.

Gerlitz, B., and B. W. Grinnell. 1996. Mutation of protease domain residues Lys37–39 in human protein C inhibits activation by the thrombomodulin-thrombin complex without affecting activation by free thrombin. *J. Biol. Chem.* 271:22285–22288.

Gomis-Ruth, F. X., M. Gomez, W. Bode, R. Huber, and F. X. Aviles. 1995. The three-dimensional structure of the native ternary complex of bovine pancreatic procarboxypeptidase A with proproteinase E and chymotrypsinogen C. *EMBO J.* 14:4387–4394.

Grinnell, B. W., J. D. Walls, and B. Gerlitz. 1991. Glycosylation of human protein C affects its secretion, processing, functional activities, and activation by thrombin. *J. Biol. Chem.* 266:9778–9785.

Hamaguchi, N., P. Charifson, T. Darden, L. Xiao, K. Padmanabhan, A. Tulinsky, R. Hiskey, and L. Pedersen. 1992. Molecular dynamics simulation of bovine prothrombin fragment 1 in the presence of calcium ions. *Biochemistry.* 31:8840–8848.

Harvey, S. C., R. K. Z. Tan, and T. E. Cheatham III. 1998. The flying ice cube: velocity rescaling in molecular dynamics leads to violation of energy equipartition. *J. Computat. Chem.* 18:726.

He, X., and A. R. Rezaie. 1999. Identification and characterization of the sodium-binding site of activated protein C. *J. Biol. Chem.* 274: 4970–4976.

Hogg, P. J., A. K. Ohlin, and J. Stenflo. 1992. Identification of structural domains in protein C involved in its interaction with thrombin-thrombomodulin on the surface of endothelial cells. *J. Biol. Chem.* 267:703–706.

Jalbert, L. R., J. C. Chan, W. T. Christiansen, and F. J. Castellino. 1996. The hydrophobic nature of residue-5 of human protein C is a major determinant of its functional interactions with acidic phospholipid vesicles. *Biochemistry.* 35:7093–7099.

Jane, S. M., L. Hau, and H. H. Salem. 1991. Regulation of activated protein C by factor Xa. *Blood Coagul. Fibrinolysis.* 2:723–729.

Kalafatis, M., M. D. Rand, and K. G. Mann. 1994. The mechanism of inactivation of human factor V and human factor Va by activated protein C. *J. Biol. Chem.* 269:31869–31880.

Kisiel, W., L. H. Ericsson, and E. W. Davie. 1976. Proteolytic activation of protein C from bovine plasma. *Biochemistry.* 15:4893–4900.

Knobe, K. E., A. Berntsdotter, L. Shen, J. Morser, B. Dahlback, and B. O. Villoutreix. 1999. Probing the activation of protein C by the thrombin-thrombomodulin complex using structural analysis, site-directed mutagenesis, and computer modeling. *Proteins.* 35:218–234.

Kraulis, P. J. 1991. MOLSCRIPT: A program to produce both detailed and Schematic plots of protein structure. *J. Appl. Crystallogr.* 24:946–950.

Le Bonniec, B. F., and C. T. Esmon. 1991. Glu-192—-Gln substitution in thrombin mimics the catalytic switch induced by thrombomodulin. *Proc. Natl. Acad. Sci. USA.* 88:7371–7375.

Le Bonniec, B. F., R. T. MacGillivray, and C. T. Esmon. 1991. Thrombin Glu-39 restricts the P'3 specificity to nonacidic residues. *J. Biol. Chem.* 266:13796–13803.

Li, L., T. Darden, R. Hiskey, and L. G. Pedersen. 1996. Computational studies of human prothrombin fragment 1, the Gla domain of factor IX and several biological interesting mutants. *Haemostasis* 26:54–59.

Li, L. P., T. A. Darden, S. J. Freedman, B. C. Furie, B. Furie, J. D. Baleja, H. Smith, R. G. Hiskey, and L. G. Pedersen. 1997. Refinement of the NMR solution structure of the gamma-carobxyglutamic acid domain of coagulation factor IX using molecular dynamics simulation with initial Ca2+ postions determined by a genetic algorithm. *Biochem.* 36: 2132–2138.

Mammen, E. F., W. R. Thomas, and W. H. Seegers. 1960. Activation of purified prothrombin to autoprothrombin or autoprothrombin II (platelet cofactor II) autoprothrombin II-a. *Thromb. Diath. Haemorrh.* 5:218–249.

Mather, T., V. Oganessyan, P. Hof, R. Huber, S. Foundling, C. Esmon, and W. Bode. 1996. The 2.8 A crystal structure of Gla-domainless activated protein C. *EMBO J.* 15:6822–6831.

McClure, D. B., J. D. Walls, and B. W. Grinnell. 1992. Post-translational processing events in the secretion pathway of human protein C, a complex vitamin K-dependent antithrombotic factor. *J. Biol. Chem.* 267:19710–19717.

McDonald, J. F., T. C. J. Evans, D. B. Emeagwali, M. Hariharan, N. M. Allewell, M. L. Pusey, A. M. Shah, and G. L. Nelsestuen. 1997a. Ionic properties of membrane association by vitamin K-dependent proteins: the case for univalency. *Biochemistry.* 36:15589–15598.

McDonald, J. F., A. M. Shah, R. A. Schwalbe, W. Kisiel, B. Dahlback, and G. L. Nelsestuen. 1997b. Comparison of naturally occurring vitamin K-dependent proteins: correlation of amino acid sequences and membrane binding properties suggests a membrane contact site. *Biochemistry.* 36:5120–5127.

Nesheim, M. E., W. M. Canfield, W. Kisiel, and K. G. Mann. 1982. Studies of the capacity of factor Xa to protect factor Va from inactivation by activated protein C. *J. Biol. Chem.* 257:1443–1447.

Nicholls, A., K. A. Sharp, and B. Honig. 1991. GRASP: graphical representation and analysis of surface properties. *Proteins.* 11:281–296.

Nishioka, J., M. Ido, T. Hayashi, and K. Suzuki. 1996. The Gla26 residue of protein C is required for the binding of protein C to thrombomodulin and endothelial cell protein C receptor, but not to protein S and factor Va. *Thromb. Haemost.* 75:275–282.

Perera, L., T. A. Darden, and L. G. Pedersen. 1999. Probing the structural changes in the light chain of human coagulation factor VIIa due to tissue factor association. *Biophys. J.* 77:99–113.

Perera, L., L. Li, T. Darden, D. M. Monroe, and L. G. Pedersen. 1997. Prediction of solution structures of the Ca2+-bound gamma- carboxyglutamic acid domains of protein S and homolog growth arrest specific protein 6: use of the particle mesh Ewald method. *Biophys. J.* 73: 1847–1856.

Reitsma, P. H. 1997. Protein C deficiency: from gene defects to disease. *Thromb. Haemost.* 78:344–350.

Rezaie, A. R., and C. T. Esmon. 1992. The function of calcium in protein C activation by thrombin and the thrombin-thrombomodulin complex can be distinguished by mutational analysis of protein C derivatives. *J. Biol. Chem.* 267:26104–26109.

Rezaie, A. R., and C. T. Esmon. 1993. Conversion of glutamic acid 192 to glutamine in activated protein C changes the substrate specificity and increases reactivity toward macromolecular inhibitors. *J. Biol. Chem.* 268:19943–19948.

Rezaie, A. R., and C. T. Esmon. 1995. Tryptophans 231 and 234 in protein C report the Ca(2+)-dependent conformational change required for activation by the thrombin- thrombomodulin complex. *Biochemistry.* 34:12221–12226.

Rezaie, A. R., N. L. Esmon, and C. T. Esmon. 1992. The high affinity calcium-binding site involved in protein C activation is outside the first epidermal growth factor homology domain. *J. Biol. Chem.* 267: 11701–11704.

Rezaie, A. R., T. Mather, F. Sussman, and C. T. Esmon. 1994. Mutation of Glu-80–>Lys results in a protein C mutant that no longer requires Ca2+ for rapid activation by the thrombin-thrombomodulin complex. *J. Biol. Chem.* 269:3151–3154.

Shen, L., and B. Dahlback. 1994. Factor V and protein S as synergistic cofactors to activated protein C in degradation of factor VIIIa. *J. Biol. Chem.* 269:18735–18738.

Shen, L., X. He, and B. Dahlback. 1997a. Synergistic cofactor function of factor V and protein S to activated protein C in the inactivation of the factor VIIIa - factor IXa complex: species specific interactions of components of the protein C anticoagulant system. *Thromb. Haemost.* 78: 1030–1036.

Shen, L., A. M. Shah, B. Dahlback, and G. L. Nelsestuen. 1997b. Enhancing the activity of protein C by mutagenesis to improve the membrane-binding site: studies related to proline-10. *Biochemistry.* 36: 16025–16031.

Shen, L., A. M. Shah, B. Dahlback, and G. L. Nelsestuen. 1998. Enhancement of human protein C function by site-directed mutagenesis of the gamma-carboxyglutamic acid domain. *J. Biol. Chem.* 273: 31086–31091.

Stenflo, J. 1976. A new vitamin K-dependent protein. *J. Biol. Chem.* 251:355–363.

Stenflo, J., and P. Fernlund. 1982. Amino acid sequence of the heavy chain of bovine protein C. *J. Biol. Chem.* 257:12180–12190.

Stryer, I. 1988. Biochemistry. W. H. Freeman and Co., New York.

Suzuki, K. 1995. Protein C. *In* Molecular basis of thrombosis and hemostasis. K. A. High and H. R. Roberts, editors. Marcel Dekker, New York. 393–424.

Tanabe, S., T. Sugo, and M. Matsuda. 1991. Synthesis of protein C in human umbilical vein endothelial cells. *J. Biochem. (Tokyo).* 109: 924–928.

Tuddenham, E. G. D., and D. N. Cooper. 1994. The Molecular Genetics of Haemostasis and its Inherited Disorder. Oxford University Press, New York.

Vijayalakshmi, J., K. P. Padmanabhan, K. G. Mann, and A. Tulinsky. 1994. The isomorphous structures of prethrombin2, hirugen-, and PPACK-thrombin: changes accompanying activation and exosite binding to thrombin. *Protein Sci.* 3:2254–2271.

Wang, D., W. Bode, and R. Huber. 1985. Bovine chymotrypsinogen A X-ray crystal structure analysis and refinement of a new crystal form at 1.8 A resolution. *J. Mol. Biol.* 185:595–624.

Yegneswaran, S., G. M. Wood, C. T. Esmon, and A. E. Johnson. 1997. Protein S alters the active site location of activated protein C above the membrane surface. A fluorescence resonance energy transfer study of topography. *J. Biol. Chem.* 272:25013–25021.

York, D. M., A. Wlodawer, L. G. Pedersen, and T. Darden. 1994. Atomic-level accuracy in simulations of large protein crystals. *Proc. Natl. Acad. Sci. USA.* 91:8715–8718.

Zolton, R. P., and W. H. Seegers. 1973. Autoprothrombin II-A: thrombin removal and mechanism of induction of fibrinolysis. *Thromb. Res.* 3:23–33.